PROCEEDINGS, 51st Workshop on Geothermal Reservoir Engineering
Stanford University, Stanford, California, February 9-11, 2026
SGP-TR-230

Cementless Geothermal Well Construction

Elvin Allahverdiyev, Khizar Abid, Catalin Teodoriu

University of Oklahoma

cteodoriu@ou.edu

Keywords: geothermal energy, well construction, cementless, well integrity, metallic packers

ABSTRACT

Geothermal wells are, by default, subjected to thermal cycles that impose demanding loads on the casing strings and cement. Historically, well construction relied on cement to provide annular zonal isolation, structural support, casing protection, and wellbore stability. However, the cement sheath is prone to mechanical failures (e.g., cracking, debonding, strength degradation, etc.) under high cyclic thermal stresses. In addition to violating environmental and safety standards, these failures can lead to inelastic buckling, sustained casing pressure, and cross-flow between communicating formations.

This work proposes a novel cementless well construction methodology to overcome the well design and integrity limitations in geothermal environments, specifically. However, the concept can be applied to any type of well application, including oil and gas, CO_2 sequestration, enhanced oil recovery (EOR), and/or underground storage wells with thorough well design and planning. The concept proposed in this work utilizes hydraulically-set metal expandable packer (MEP) systems as an alternative to cement for the annular zonal isolation. These packers need to be set at competent formations for a long-lasting metal-to-rock and metal-to-metal seal. This work presents a model with the key design considerations for a successful application using a commercial well design software that also has finite element analysis (FEA) features. In order to eliminate packer failures, certain pre-tension is applied to the strings after each packer set. The concept offers very high potential to achieve maximum well integrity over a longer operational life-of-well, even post-plug and abandonment, neglecting the corrosion damage, which needs further solution development. The metallic packer technology already has a proven track record in the oil and gas wells with back-up cement in place.

1. INTRODUCTION

Research objectives of the alternative energy and decarbonization goals have recently pushed by the energy transition goals. While some focus heavily on the hydrogen (Abdullah and Sajjadi 2024), carbon capture and storage (Baig et al. 2025, Hajiyev et al. 2025), geothermal energy, as well as the working fluid selection in geothermal wells (Fentaw et al. 2026), this study is dedicated to solving the well integrity challenges of geothermal wells to save the long-term asset investment. According to expert opinion, the best solution for minimizing well integrity problems is during the well construction process. Since the early days of drilling, cement has been adopted as the most preferred wellbore annular isolation method for better well integrity assurance. Studies by various authors have shown that the integrity of well barrier elements is significantly affected by cement, leading to interfacial leakage pathways at the casing-cement interface. It has been shown that cement fails earlier than steel pipe strings in critical wells, especially under tension. Engineered cement with very low Young's Modulus and high tensile strength is proposed as an alternative, but it is difficult to achieve in practice. Only a few alternatives to wellbore cement solutions have been economically imposed on the market. Additionally, the cement manufacturing process is highly CO2-intensive (Teodoriu et al. 2021, Teodoriu et al. 2022).

The narrow-margin PPFG (pore pressure fracture gradient) formations also create additional challenges regarding the cement placement ECDs (equivalent circulating density), and borehole integrity issues. In the case of slimhole well construction, the thin cement cannot serve as a strong interface barrier as defined by the current industry standards. Thus, this new solution can also be applied to the slimhole well concepts (Teodoriu et al. 2021, Teodoriu et al. 2022).

Hydraulically activated external casing packers, which serve as metallic wellbore-isolation solutions, are reliable alternatives to cement. These tools can be rotated while running in a hole, expand to high diameters, conform to the wellbore geometry, and isolate differential pressures above 15,000 psi (Teodoriu et al. 2021). Metal expandable packers (MEP) can enable cementless annular isolation across highly layered formations, replacing traditional cementing plans and improving efficiency. These were introduced back in 2010 to create a reliable, well annular barrier (WAB) offering a reduction in the use of cement and mitigation of sustained casing pressure (SCP) (Teodoriu et al. 2021). Fig. 1 below shows a classic application of the MEP in horizontal multilateral well concepts. The MEP sleeve is manufactured from a high-ductility alloy that hardens as it strains, allowing uniform expansion that conforms to the borehole shape while accounting for irregularities. Controlling the contact stress between the MEP and the borehole formation can allow seal capability in the worst-case borehole geometries (ISO 14310 Std.). Several in-house qualification tests have been successfully performed (per ISO 14310/API 11D1 testing protocols) and validated using FEA studies (Teodoriu et al. 2021, Teodoriu et al. 2022).

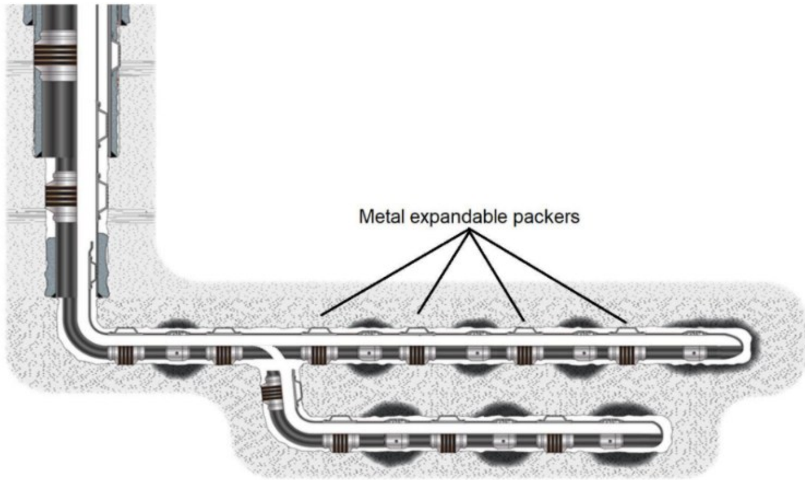

Figure 1: Multilateral well concept – MEP used for well construction and zonal isolation (Teodoriu et al. 2021).

The proposed design concept is to place MEPs at every stable formation to reduce the crossflow, while ensuring that they are set only in the competent formations. In addition, the packers will be set at the casing shoe between the outer and inner strings to eliminate SCP. This solution could enhance the well construction process as well as achieve maximum well integrity for a much longer period of time compared to the cement. The MEP setting can also be achieved in challenging zones of potential cement losses and does not depend on the subsurface fracture gradient, ensuring that the casing is run to the desired shoe depth. Moreover, emissions per well could be reduced through this novel concept (Teodoriu et al. 2021, Teodoriu et al. 2022).

One concern when eliminating cement would be buckling, but with the use of shorter MEPs and centralizers, this can be solved. Nevertheless, pre-stressing of the upper free casing is the best solution to avoid buckling during thermal expansion, if any (Teodoriu et al. 2021, Teodoriu et al. 2022).

2. GEOTHERMAL WELL INTEGRITY ISSUES

2.1 Longevity of Zonal Isolation and Cement Integrity

The need for cement in well construction is mainly given by its following functions (Teodoriu et al. 2022):

- To seal cross flow and block fluid movement in the vertical direction (i.e., low permeability and porosity):
  - to displace the mud and uniformly occupy the annular space,
  - to keep the fluids from expanding in the annulus.
- To support casing (especially the surface casing) and provide mechanical support to impede axial movement:
  - to hold the casing string in place and avoid buckling,
  - to create a strong bond with the formation and casing.
- To protect casing from corrosive fluids that may exist in the porous formations:
  - long-term resistance to downhole conditions.

Generally, there are three mechanical failure modes for the cement. These are cement radial cracking (Fig. 2a), plastic deformation (Fig. 2b), outer and inner debonding (Fig. 2c and Fig. 2d) (Ugwu 2009, Petty et al. 2003). Radial cracking occurs when the cement is in fatigue mode (Phi et al. 2019).

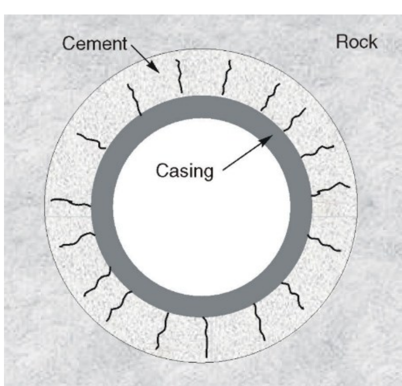

a)

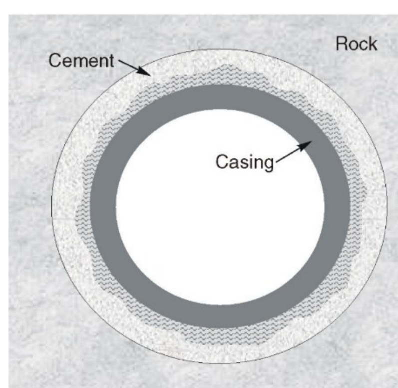

b)

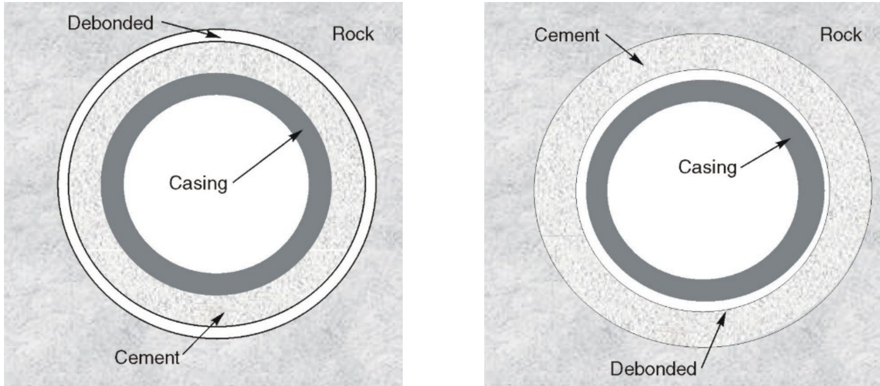

c) d)

Figure 2: Typical failure modes in cement: a) cracking, b) plastic deformation, c) cement-formation interface debonding, d) casing-cement interface debonding (Petty et al. 2003).

It has been found that the heat transfer from formation to casing (i.e., formation temperature > casing temperature) is comparatively more detrimental to cement integrity than the opposite scenario, where the casing temperature is higher than the formation temperature (Wu et al. 2020, Wu et al. 2021). Though, regardless of the heat transfer direction, radial and hoop stresses in cement have higher sensitivity to temperature changes compared to pressure loads (Wu et al. 2020).

Undergoing geothermal temperatures means the introduction of tensile stresses in the cement and compressive stresses in the casing (Southon 2005). According to the work of Berndt and Philippacopoulos (2002), Liu et al. (2025), fiber-reinforced cements withstand higher tensile stresses than conventional cements and have better sealability in geothermal wells. Radonjic and Bello (2015) also concluded that long, uneven glass fibers can be used to reduce permeability in the wellbore cement sheath. An operator developing a geothermal field (where the BHT ranges between 250-300℃) in Indonesia found the wells suffering from various well integrity issues due to structural failure of the conventional cement sheaths, as well as due to ineffective slurry placement. It has been recognized that the structural damage to the cement sheath is typically in the form of debonding, cement sheath cracking, and/or compressive shear. Therefore, elastic cement systems were used that incorporate various mechanical property enhancement additives (Ravi et al. 2008).

The acid fluids formed from wet CO_2 and H_2S (Yin et al. 2024) can attack the cement sheath and corrode the casing exterior. This can also be triggered by hydraulic stimulation operations combined with thermal cycles, which deteriorate the cement integrity (Petty et al. 2003).

Cement undergoes strength degradation when exposed to geothermal temperatures for extended periods. Above the critical temperature of 104-160°C, its strength will decrease with increased temperature and age (Carter and Smith 1958, Saunders and Walker 1954). Silica flour (or fly ash) has been suggested to be used as a cement stabilizing agent under high geothermal temperatures to combat strength retrogression (Bett 2017, Teodoriu et al. 2022). However, carbonation of the silica causes the cement to develop high porosity rapidly (Hole 2008a, Patel et al. 2025). Also, silica cement composite does not eliminate the issues related to CO_2 and H_2S attacks (Arbad et al. 2022). The addition of steel and glass fibers, along with silica flour, would be necessary to increase the cement sheath's durability in geothermal environments (Radonjic and Bello 2015).

Nowadays, the research and development focus has shifted to introducing self-healing properties in cement (e.g., Pyatina et al. (2016), Sugama and Pyatina (2019), Pyatina and Sugama (2022) developed thermal shock-resistant cement (TSRC)). Pozzolans help to hydrothermally self-heal damaged cementitious composites at 300°C (Pyatina and Sugama 2020). While acknowledging the recent development in the cement industry, Madirisha and Ikotun (2025) listed the limitations of these alternative cementitious systems for geothermal wells as follows:

- TSRC: poor stability in acidic environments,
- Calcium phosphate cement (CaP): weak performance in strongly acidic and thermal cycling conditions,
- Sodium silicate-activated slug (SSAS): degrades under high CO_2 or mixed chemistries.

Many researchers have concentrated their efforts on creating new cement recipes that can withstand high geothermal temperatures. A closer examination of the geothermal wells revealed that the primary load on the cement is caused by casing expansion. According to the numerical and experimental works of Lambrescu et al. (2021) and Lambrescu and Teodoriu (2022) on cement bonding, the overall debonding force is not sensitive to the cement's Young's modulus and Poisson's ratio, and a post-debonding frictional force exists that can still hold the casing in place (Teodoriu 2021). However, a leak path would have formed before debonding (Lambrescu and Teodoriu 2022). Abid et al. (2025) also confirmed that a leak path can form well before the cement undergoes debonding failure and concluded that repeated thermal cycles significantly reduce debonding strength. Teodoriu and Lambrescu (2023) showed that tensile (Type I) failure is the most critical debonding mode during cooling scenarios in geothermal wells and can initiate with a relatively small temperature change of only 60°C. Whereas Lambrescu et al. (2024) concluded that Type II (shear) debonding dominates during heating. Later, it was found that during cooling, even a very low ΔT of 10°C may cause debonding because the cement's IBTS (interfacial bonding tensile strength) is typically much lower than its shear strength (Lambrescu et al. 2024). It has also been argued by Lambrescu et al. (2024) that even a very high cement bond strength (i.e., IBSS [interfacial bonding shear strength] of 4 MPa – which is highly unlikely to be achieved with current technology) is not enough to mitigate debonding under high differential temperatures (e.g., a ΔT of 265°C). Lambrescu et al. (2025) also concluded that the casing-cement interaction will continue to hold the casing expansion post-debonding.

Lian et al. (2020) evaluated the continuous leak paths in the cement sheath in hydraulically fractured wells. This can be of specific interest for EGS (enhanced geothermal system) wells, and it has been found that multistage fracturing causes cumulative plastic strain and micro-annulus at the casing-cement interface (Xi et al. 2022). They also concluded that the accumulated plastic strain does not create significant internal cracks in the cement, but rather at the casing-cement interface. When the cyclic stresses exceed the cement's dilatancy yield stress, its permeability increases and creates another leak path (Lian et al. 2020). Jiang et al. (2020) also conclude that the most effective method to reduce the risk of debonding is to increase the critical normal strength and shear strength of the cement-casing interface. Santos and Dahi Taleghani (2022) recognized that poor bonding leads to a much faster pressure build-up. The work conducted by Gu et al. (2022) concluded that the micro-annulus size increases as the casing pressure reduces (e.g., production) and decreases as the pressure increases (e.g., injection). Gu et al. (2024) also concluded that the cement-formation interface is more prone to debonding than the casing-cement interface in the injector wells, and high fluid temperature, flow rate, viscosity, and casing pressure increase the fracture propagation pressure and reduce debonding risk. If the cement is brittle, the number of cracks that the cement experiences may increase (Pyatina and Sugama 2020). An additional challenge related to cementing in thermal wells is that the linear coefficient of thermal expansion (LCTE) of the API grade OCTG is different than that of the conventional well cement solutions (13×10^{-6}/°C for steel and 8×10^{-6}/°C to 10×10^{-6}/°C for cement), whereas using a low-LCTE metal such as titanium is not economically attractive (Johri et al. 2025). Xu et al. (2018) also concluded that in order to protect the cement sheath, the casing wall thickness, LCTE, and the cement sheath elasticity modulus need to be decreased, while the fracturing fluid temperature should be increased. Johri et al. (2025) also suggested the use of a thermally responsive cement (TRC) system to mitigate the encountered challenges.

Since the early drilling, cement was adopted as the most preferred wellbore annular isolation method for better well integrity assurance. Studies by various authors have shown that the integrity of well barrier elements is significantly affected by cement, leading to interfacial leakage pathways at the casing-cement interface. It has been shown that cement fails rather earlier than the steel pipe strings in critical wells, especially under tension, and engineered cement with very low Young's Modulus and high tensile strength is proposed as an alternative (Johri et al. 2025, Tomilina et al. 2012, Garnier et al. 2008). Continuous improvement in cement should not be discontinued; however, only a few alternatives to wellbore cement solutions have been economically presented in the market. In addition, these implementations are still difficult to achieve in practice. Maharaj (1996) reported that 15% of casing failures in a mature thermal field were due to buckling of a poorly cemented casing string. It is worth noting that there are still a lot of factors related to cementing that can go wrong (e.g., casing decentralization, inadequate mud removal, incomplete cement placement, inadequate cement interface bonding, contamination, lost circulation, etc.) while cement gels and loses its hydrostatic pressure. These complications can easily lead to sustained casing pressure in geothermal wells. Another example of potential problems with cementing geothermal well casings may also include the build-up of a thick filter cake (Salim and Amani 2013, Allahvirdizadeh 2020). Allahvirdizadeh (2020) also noted that cementing can account for up to 15% of geothermal well construction activities.

2.2 Sustained Casing Pressure and Casing Deformation

Based on the investigation of the failure modes in 136 geothermal production wells in Iceland, Ford et al. (2017) reported the distribution shown in Fig. 3.

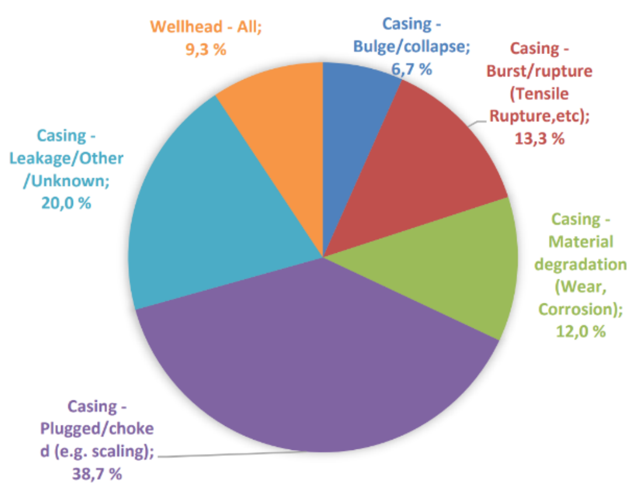

Figure 3: Failure mode distribution in 136 geothermal producers in Iceland (Ford et al. 2017).

Historically, cementing all the casing strings to the top has been necessary to minimize the steel failures due to thermal expansion during production and the presence of trapped fluids behind the strings (Saito 1994). The trapped fluid expands during production and can produce pressures up to 45-50 psi/°F, inducing burst or collapse failures (Arbad et al. 2022) (1.6 MPa/°C at temperatures above 100°C (Hole 2008b)). The trapped fluid between the casing strings causes failures more often than other reasons (Arbad et al. 2022). Since all the casing strings must be completely cemented (Union 2016), casing-cement-formation interface bonding becomes very critical for maintaining long-term well integrity. Even if a small volume of excess water entrapment occurs, the AFE (annular fluid expansion) during production can induce collapse of the inner string (Union 2016).

The sustained pressure due to the trapped fluids holds a significant share of the casing collapse failures in geothermal wells. It has been predicted that these failures should occur in the pipe body rather than near the couplings, as the trapped fluids occupy less annular space at the couplings (Southon 2005).

In the subsea wells, the B- and C-annulus cannot be monitored. However, nowadays, the industry has driven to develop technology for B-annulus monitoring. APB (annular pressure build-up) is bled off with the needle valves in the subsea wells, and when it cannot be bled, it is called sustained casing pressure (SCP).

Based on a detailed investigation of the production wells in the Gulf of America, GHG (2006) found that up to 60% of wells had casing pressure problems (i.e., sustained casing pressure, even up to 70% of wells affected), which were related to the poor well completions and inadequate casing-cement-formation interface bonding (GHG 2006). Further statistics indicated that 33% of problems were directly linked to cementing. Based on the report, the main cementing problems that could cause SCP were (GHG 2006):

- micro-annuli caused by expansion/contraction,
- channeling due to improper mud removal,
- lost circulation into fractured formations,
- flow after cementing,
- mud cake leaks,
- tensile cracks in cement due to pressure and temperature cycles.

Based on other references (Muehlenbachs 2011, Vengosh et al. 2014), about 43% of 15,000 tested wells in the Gulf of America have shown SCP due to cement damage, more than 50% of which exists outside the production casing (Liu et al. 2018). Based on feedback from operators in the Marcellus shale, 25% of the wells show SCP (Liu et al. 2018, Williams et al. 2011). Another example could be the Fuling shale gas field in China, where the percentage of wells with SCP issues reached as high as 86%, 71% of which was between the production-intermediate casing annulus (Liu et al. 2018). Although it may be argued that geothermal wells do typically not have the high-pressure conditions making the SCP issue critical, the main design philosophy behind EGS is to perform hydraulic fracturing. Thus, it is a good idea to identify the root causes of the SCP based on the lessons learned from the unconventional hydrocarbon developments.

SCP is the pressure observed in the casing annulus that returns after bleed-down (Yao and Wojtanowicz 2017). According to Yao and Wojtanowicz (2017), it is not the result of thermal effects. The problem is large and affects 8,122 wells and 11,498 casing strings in the OCS (Outer Continental Shelf). 50% of SCP cases occurred in the A-annulus. Bureau of Safety and Environmental Enforcement (BSEE) procedure for the regulatory evaluation of sustained casing pressure on fixed offshore platforms suggests that the leak rate is large if the 24-hour pressure build is equal to the original pressure. In other words, the pressure should be less than the maximum allowable wellhead operating pressure (MAWOP) and be possible to be bled to 0 psi. According to this procedure, MAWOP is calculated as the lesser of (Yao and Wojtanowicz 2017):

- 50% of burst for the casing string in question, 75% of collapse of the inner casing string, 80% of burst of the next outer string,
- or if there is no outer string, 30% of burst for the string in question, 75% of collapse of the inner string.

One of the main problems causing casing collapse in geothermal wells is APB. Some measures suggested by Lentsch et al. (2015) to avoid collapse due to APB were:

- allowance for leak-off to formation,
- increased compressibility of the annulus contents,
- reduced volume of entrapped fluids,
- increased casing collapse rating,
- slow heat-up during production.

It is worth noting that many authors have not considered the poromechanical behavior of cement at ultra-high temperatures. (Vu et al. 2020) discussed what could take place concerning its pore pressures when a cement sheath is heated to high temperatures. The high pore pressures created under these conditions can cause a micro-annulus at the boundary of the cement sheath (Vu et al. 2020).

Based on the experimental and numerical research, Zhang et al. (2024) concluded that the cement sheath and its interfaces serve as weak points for potential integrity failures in geothermal wells. One of the main conclusions was that the cement interface leaks and loses its sealing capabilities at high temperatures (e.g., 300°C).

Based on the investigations of 136 production well failures in Iceland's geothermal fields, Ford et al. (2017) reported that casing-to-casing trapped annulus fluid pressure led to not only the rupture and collapse failures, but also choking the well more than 50% in some cases. Statistically, a higher number of failures occurred in the shallower zones of the wells (less than 500 m) where the compressive thermal stresses were greatest. They also noted that if the trapped-water location in the uncemented pockets has formation outside it, the casing will almost certainly not collapse. This is a long-standing design philosophy for the multi-string casing design in the industry that allows leak-off to the formation fracture gradient, by which the pressure is bled off into the formation in case of build-up. It is a good practice to ensure that the casing collapse rating is higher than the fracture gradient in impermeable formations (or the pore pressure in the case of permeable formations) to avoid the negative differential pressure building up.

A compressible spacer can compensate for the fluid expansion. However, one of the main challenges is to properly place the fluid in the annulus. Another concern with these is the question of the stability of the spacer in terms of physical properties (Lentsch et al. 2015). Another solution would be to wrap the casing with crushable foam to provide volume that is not cement. This volume can compensate for the fluid expansion. However, it is a very fragile design and can be challenging to run in a deviated well (Lentsch et al. 2015).

2.3 External Casing Corrosion

Several investigations over hundreds of geothermal wells in the Pacific-South East Asia region by Southon (2005) noted external corrosion evidence on the production casing strings after 5 years, where the corrosive fluids penetrated along the micro-fractures in the cement. To be noted, this can occur at any depth along the production casing (Southon 2005). Even if the casing strings are completely cemented, there is still a good chance that the corrosive fluids can migrate through the cemented annular space and corrode the steel, even with API high sulfate-resistant Class G cement (Southon 2005). According to Southon (2005), internal corrosion was not a typical problem in the investigated geothermal wells. The working fluid in geothermal wells often contains CO_2, which occurs naturally. Since CO_2 forms carbonic acid and attacks the cement, the cement loses its strength. Ahmed et al. (2022) evaluated hydroxyapatite-based (HOAP) cement for geothermal well applications and concluded that HOAP cement has better resistance to carbonic acid. According to Shadravan et al. (2015), two major hydration products of cement used in geothermal wells are calcium silicate hydrates (CaO-SiO_2-H_2O) and calcium aluminum silicate hydrates (CaO-Al_2O_3-SiO_2-H_2O), which are very susceptible to CO_2 corrosion and deteriorate cement. Another corrosion agent in geothermal wells can be sulfuric acid (H_2SO_4), which can lead to internal cracks (Shadravan et al. 2015, Yin et al. 2025) and swelling in the cement sheath (Shadravan et al. 2015).

To summarize the previously mentioned limitations of a cemented well construction philosophies especially the number of cycles it would take for cement to fail in critical geothermal applications, a new design methodology is proposed in this study. The proposed design philosophy is to replace cement with several MEP components and thus have better control over the geothermal well lifecycle management. Although buckling and inelastic deformation concepts are not emphasized at this moment, further evaluations incorporating the post-yield design methodology will be made in a separate study. The main motivation behind this radical shift towards the cementless philosophy was the fact that a debonded casing-cement interface is already a severely compromised well integrity barrier, leading to buckling, SCP, and collapse failures.

3. DESIGN PHILOSOPHY

The validation model used data primarily from the Utah FORGE data repository to assess the suitability of the cementless well construction and completion design, aiming to build the most appropriate design case for geothermal applications environments. Fig. 4 shows the trajectory of the well used in this study, which actually belongs to FORGE 16B. The study is divided into two parts, where one evaluates the application for a high-temperature EGS application, while the other pushes the limits for a supercritical hydrothermal application where there is no hydraulic fracturing involved.

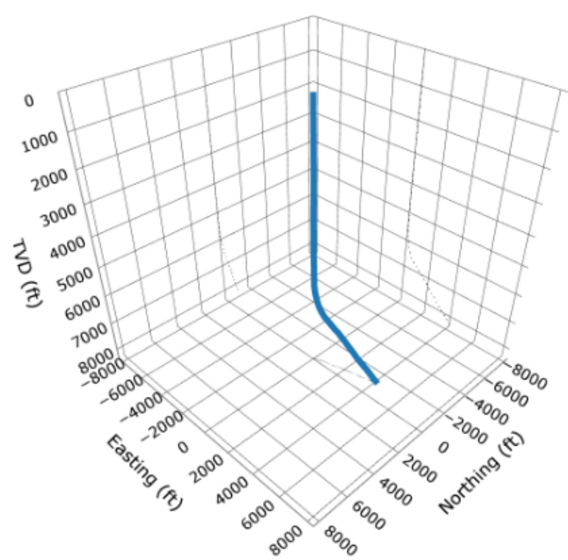

Figure 4: FORGE 16B well trajectory.

3.1 High-Temperature EGS Application

Fig. 5a shows the formation tops data, which are denoted as Basin Fill and Granitoid, while Fig. 5b presents the UDT (undisturbed temperature gradient) belonging to the FORGE subsurface (Subsurface Data 2025).

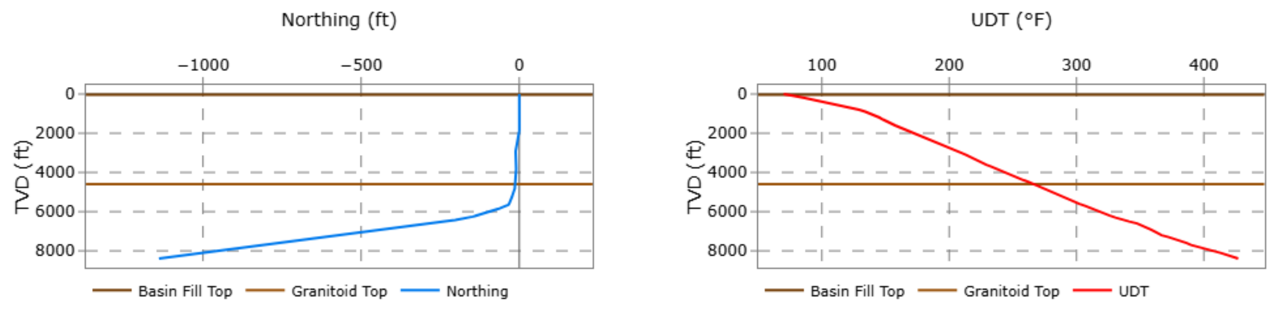

Figure 5: a) Formation tops, b) UDT.

Table 1a shows the well configuration representing well 16B (conductor was ignored in this design study), while Table 1b shows the DFs (design factors) utilized. It should be noted that the connections for the surface and intermediate casings were originally chosen as BTC in the FORGE site (Allahverdiyev et al. 2025). However, in this study, they have been changed to be proprietary. As can be expected from the DFs, the working stress design model was utilized in this analysis. Though it is understood that the failure criteria with the help of isotropic materials' plastic deformation theory may also be suitable to assess concepts such as post-yield criteria, strain-hardening, or -softening, and the number of cycles that the steel material can effectively endure using the hysteresis plot.

Table 1: (a) Well configuration, modified after McLennan et al. (2023), (b) geothermal casing minimum design factors (Unit 2016, Zealand 2015).

a)

String	**OD (in)**	**Weight (ppf)**	**Grade**	**Connection**	**TOC**
Surface	16	84	JFE-110T	TSH Blue Max Dopeless	Surface
Intermediate	11 ¾	65	JFE-125T	TSH Blue	Cementless
Production	7	38	P-110EC	VAM 21 HT	Cementless

b)

DF	
Triaxial-Burst	1.25
Axial-Tension	1.80
Axial-Compression	1.40
Uniaxial-Burst	1.50

Table 2 in the Appendix lists the operational details for the post-installation and life-of-well load cases with the WHT (wellhead temperature) and WHP (wellhead pressure) values. The data were again mostly obtained from the FORGE data repository, which was very useful for conducting a comparable numerical analysis with the cemented design. For the surface inlet temperature of the injection operations, it may raise questions why it has been chosen to be 90°F. The reason behind this is to potentially reduce the damage from tensile cycles. This temperature value has been identified as reasonable and used in the simulations because the stimulation operations will require cold inlet temperatures to induce hydraulic fracturing. However, if possible, pre-heated water with the maximum possible surface temperature should be used. However, using a 90°F inlet temperature for the stimulation operations makes this study relatively more conservative for evaluation. For the steady-state life-of-well operations, it has been assumed that all 5 stages of the downhole injection zones are fully functional and have 100% cluster efficiency, and the pump-in and flowback operations have been specified to be 20 years. It is important to note that initial conditions for the cementless casing strings can reasonably be assumed to be the casing running temperature profile with an added circulation possibility before setting and pre-tensioning the packers. This would also help reduce the range of compressive-tensile cycling. In this study, it was assumed to be just the casing running temperature profile for the cementless casing strings. In addition to the long-term injection-production operations, well construction phase thermal results were also obtained, as shown in Fig. 6a, 7a, and 8a for the surface, intermediate, and production casing strings, along with the current stage well schematic in Fig. 6b, 7b, and 8b.

As can be seen from Fig. 8b, multiple packers have been specified in the openhole sections for the 7" production and 11 ¾" intermediate casing strings, while one last packer was specified inside the previous shoe. These are metal expandable packers (MEP), and there is an expandable anchor (WEA) element at the intermediate casing shoe, which is compatible with the MEPs. A beneficial feature that may be incorporated into this system is the control line feedthrough, which may be useful for corrosion inhibition and needs further risk assessment study. An argument can be made that the geothermal wells already undergo corrosion at both the internal and external (i.e., if the cement cracks or debonds) profiles of the casing strings, with corrosive geothermal fluids. Fully cemented strings may be another factor limiting the management of external profile corrosion.

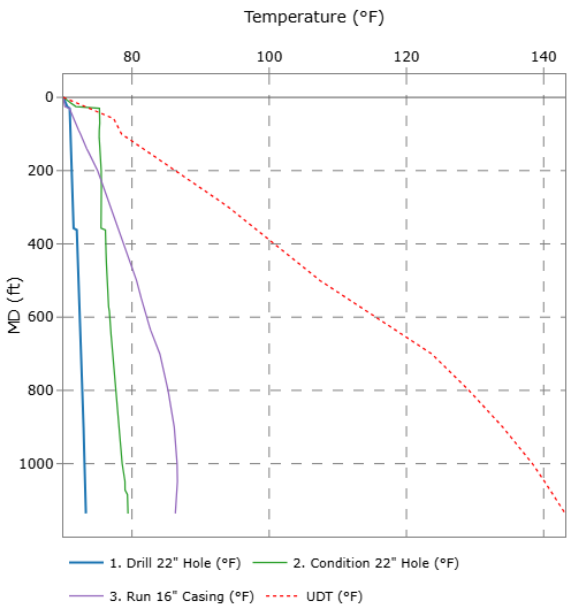

a)

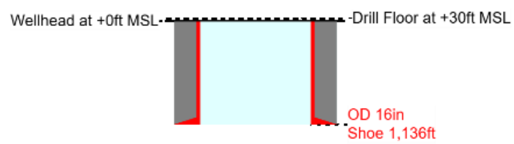

b)

Figure 6: 16” cemented casing: a) well construction phase thermal results, b) current stage well schematic.

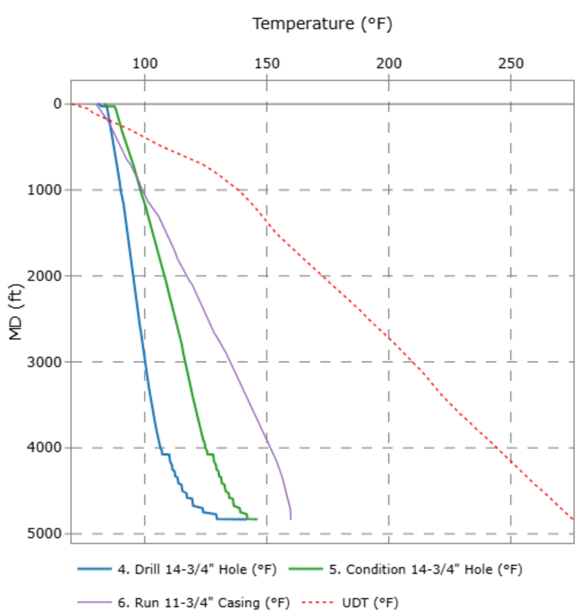

a)

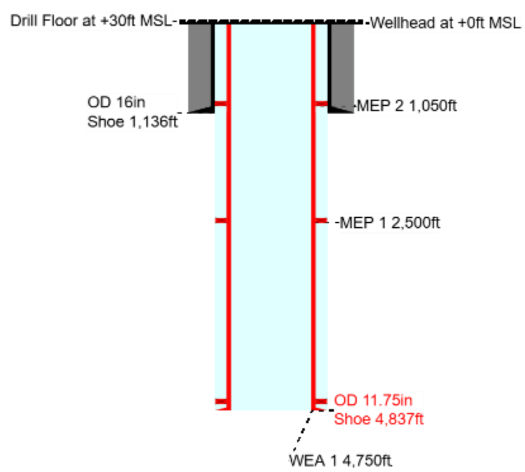

b)

Figure 7: 11 ¾” cementless casing: a) well construction phase thermal results, b) current stage well schematic with WEA[1], MEP[1], and MEP[2].

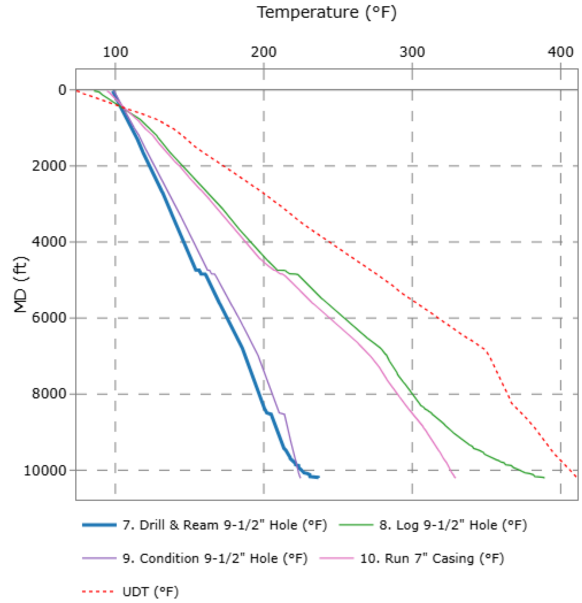

a)

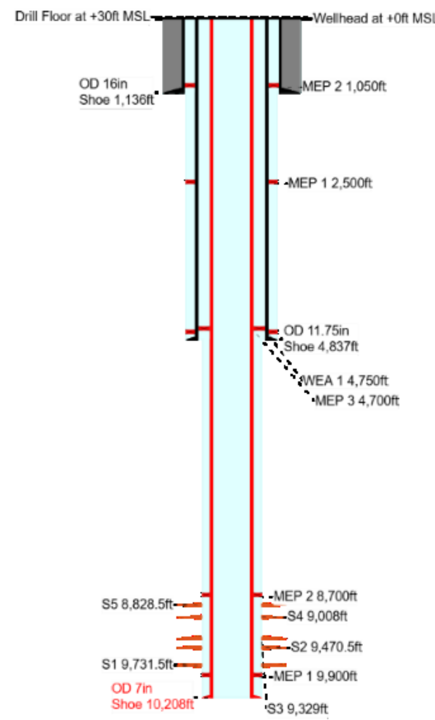

b)

Figure 8: 7" cementless casing: a) well construction phase thermal results, b) current stage well schematic with MEP[1], MEP[2], and MEP[3].

Fig. 9 presents the temperature results across the 7" pipe body, from which it can be seen that the most dominant thermal operations are SS (steady-state) flowback and pump-in. Although it is not typical that both long-term (20 years) injection and production operations will be performed in a single well in an EGS application, these were assumed to happen in the same well for added conservatism. At the same time, Fig. 10 presents the pressure results for the corresponding operations.

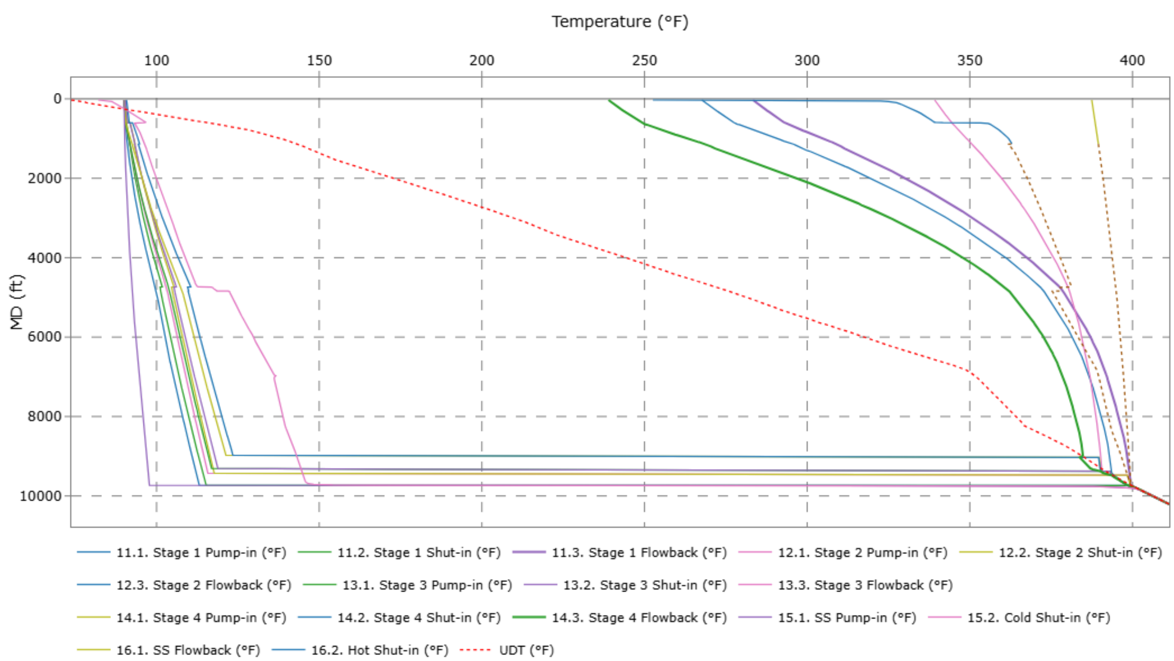

Figure 9: 7" cementless casing well completion phase thermal results.

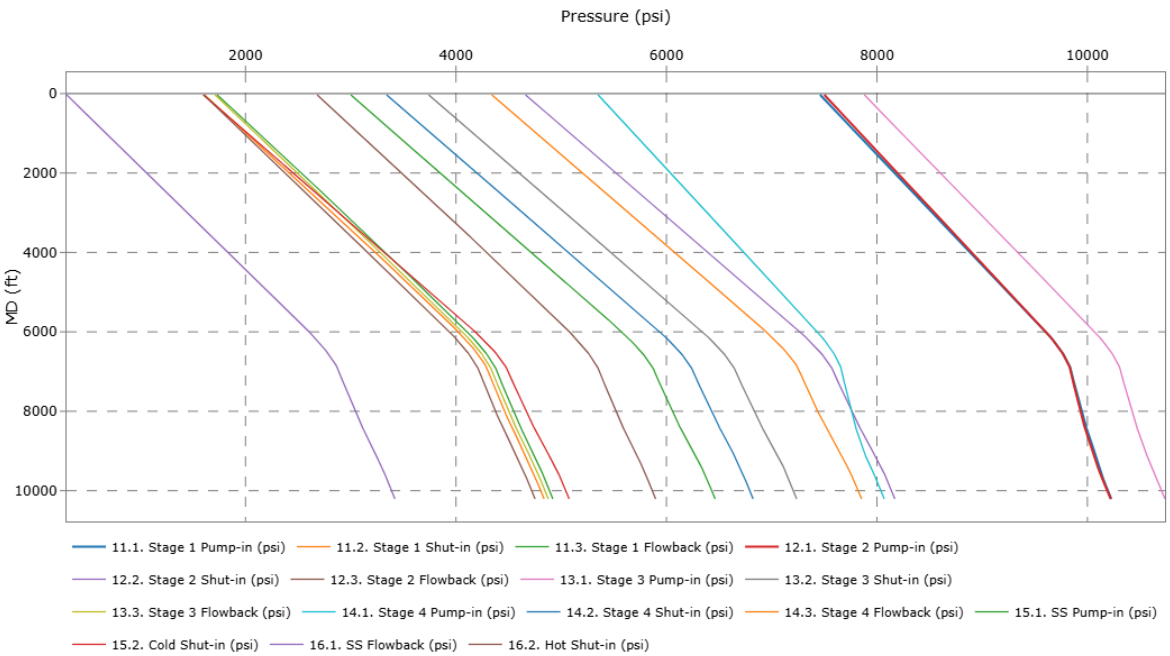

Figure 10: 7" cementless casing well completion phase hydraulic results.

3.2 Supercritical Hydrothermal Application

In addition to the high-temperature EGS design methodology, which had the UDT belonging to FORGE downhole conditions, an additional assessment has been made concerning the supercritical conditions (Fig. 11). However, due to the range of the compressive-tensile load cycles, it has been decided to move forward with the natural supercritical hydrothermal reservoirs, which may not require hydraulic fracturing. Table 3 in the Appendix presents the operational details, assuming the WHT and WHP values. The design was essentially kept the same, while the UDT was changed to be 650°F at the well TD (total depth) to represent the near-supercritical conditions. Although the main idea was to eliminate hydraulic fracturing in this analysis, quenching cannot be permanently removed from the well life cycle, as these resources would be hydrothermal. Therefore, controlled quenching was modeled using a 90°F inlet temperature, relatively short operational durations, and 5-15 bpm flow rates. Instead of hydraulically fracturing different stages, the same clusters have been assumed to be just perforated.

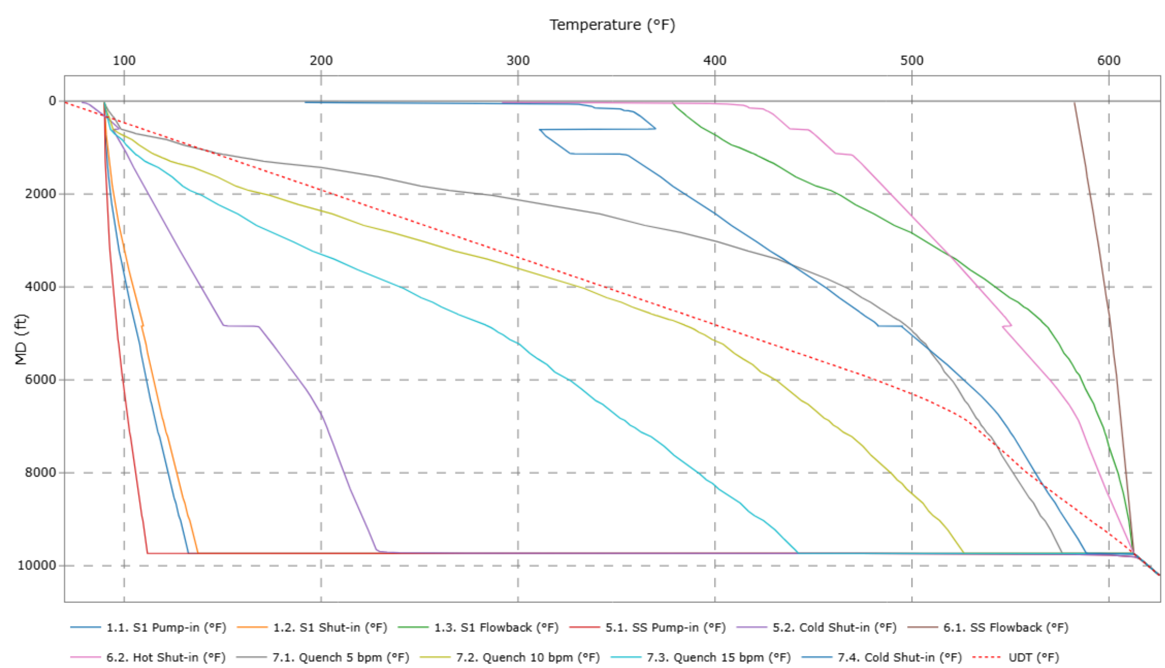

Figure 11: 7" cementless casing well completion phase thermal results.

4. RESULTS

4.1 High-Temperature EGS Application

Fig. 12 presents the results for the packer elements with no applied pick-up (PU) or slack-off (SO) forces. It can first be seen from Fig. 12d that the VME (von Mises equivalent) design limits plot (DLP) is fairly conservative for the 7” string with the chosen DFs and under such operating conditions where the bottomhole temperatures (BHT) are relatively high (i.e., 427°F). In fact, the casing still shows a conservative DLP for the cemented 7” string as well (Allahverdiyev et al. 2025). Fig. 12a shows the packer operating envelope (POE) for the MEP[1], which is set at 9,900 ft MD (measured depth) just below the S_1 (stage 1) in well 16B, while Fig. 12b is for MEP[2] placed just above the S_5 at 8,700 ft MD in the same well. There is also a third MEP placed inside the previous 11 ¾” intermediate casing at 4,700 ft MD, and its POE is shown in Fig. 12c. A few observations can be made from these envelopes regarding the operating conditions. The lowermost MEP[1] is set across a relatively hot formation interface, where the injection operations’ cool-down temperatures may not effectively reach this packer. This helps to ease the tensile cycles for this packer compared to the one shown for MEP[2]. Where the tensile loads due to S_1 pump-in, S_2 pump-in, S_3 pump-in, and S_4 pump-in load cases are marginal with the assumed POE. Since MEP[3] is placed at a relatively shallow depth where the difference between the UDT and the cold injection and hot production load cases does not induce much tensile and compressive stress, the axial tubing-to-packer (T_2P) forces do not exceed 200 klbf.

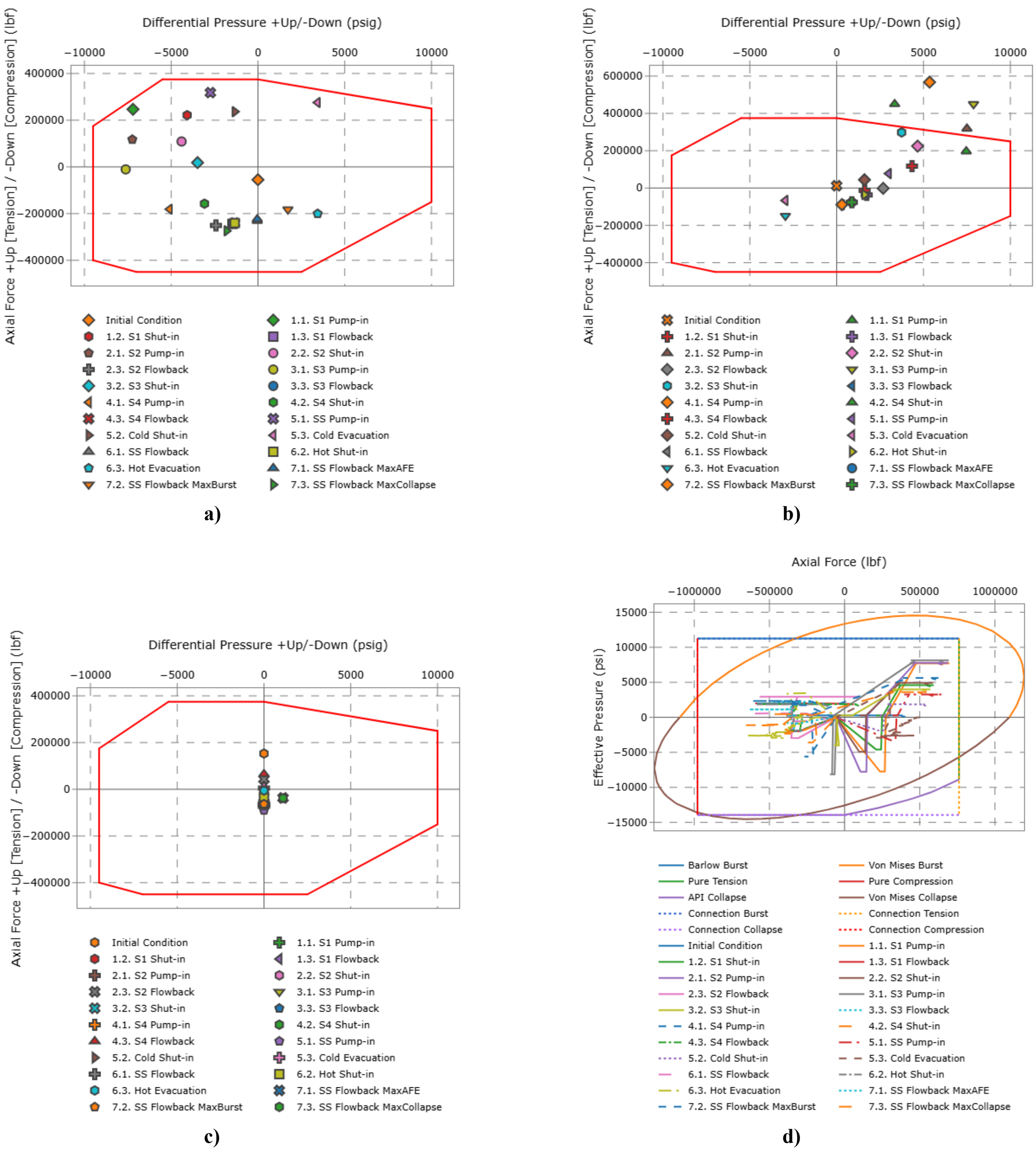

Figure 12: 7” cementless casing (no PU/SO): a) MEP[1], b) MEP[2], c) MEP[3], d) DLP.

From the first assessment, it looks like the MEP² can benefit from an SO load, while the MEP³ may allow up to 200 klbf PU load for pre-tensioning. It was decided to apply 200 klbf SO and 220 klbf PU loads on MEP² and MEP³, respectively, and lock them in between the packers. The applied SO is controversial due to buckling forces, as this cementless application would require only PU forces to avoid cases where sinusoidal or helical buckling loads exceed the effective force. This means that the MEP² should have a higher axial capacity rating around 600 klbf tensile capacity, as previously shown in Fig. 12b. The resultant POEs for MEP² and MEP³ are shown in Fig. 13a,b, respectively. Since the difference between the applied PU and SO loads is not too big (i.e., a resultant load of 20 klbf PU), it is not surprising to view the DLP (Fig. 13d) with the load cases not pushed significantly to the tensile limits, though there is still some room for more tension. Fig. 13c shows that the buckling loads exceed the effective forces even inside the pipe-in-pipe string section. Alternative solutions to eliminate or effectively reduce buckling loads would be using centralizers or guides. However, a separate dedicated study must be made to identify if these centralization tools can reliably provide the equivalent restraint, considering the limited number of them being installed. Another alternative would be to set an additional number of mini-packer systems to effectively reduce buckling. It should also be noted that Fig. 13c shows the worst-case scenario, where buckling happens during the 'SS Flowback MaxBurst' load case, which also incorporates the annular fluid expansion (AFE) concept. Proper attention was given to model the pressure build-up due to AFE.

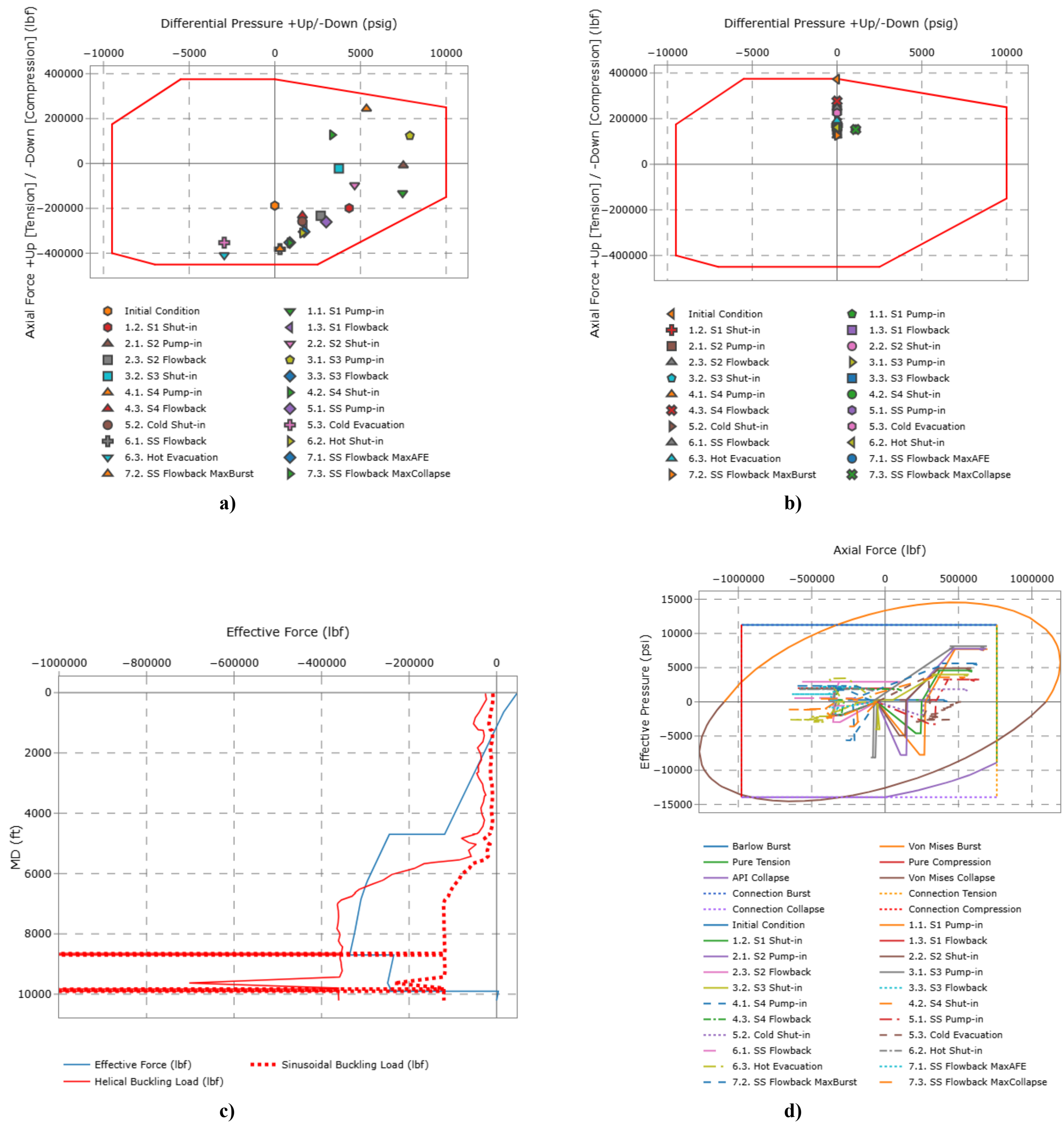

Figure 13: 7" cementless casing: a) 200 klbf SO on MEP², b) 220 klbf PU on MEP³, c) buckling summary, d) DLP.

Since the highest temperatures were observed during the SS flowback operation, it was used as the reference final operation for the analysis, and all three loading conditions were incorporated: the maximum burst occurs when the external pressure profile is default and the pressure build-up acts inside the string. The maximum collapse condition occurs when the flowback pressures act within the string, while the pressure build-up acts between the external profile and the formation. The AFE considers both burst and collapse loads. It is worth noting that a 600 ft N_2 (nitrogen) cap was simulated to reduce the amount of pressure build-up in the pipe-in-pipe (7” x 11 ¾”) section (i.e., incremental volume of 38.3 bbl), whereas the pressure build-up in the pipe-in-hole section was modeled to leak off into the formation fracture gradient, and the remaining pressure build-up was considered to act as a collapse load. This approach helped the AFE load cases stay inside the envelope (Fig. 13d).

Fig. 14a,b show the POEs for the annular isolation packers and an anchor component set in the 11 ¾” casing. It was decided that the string can also benefit from a WEA[1] (expandable anchor) component (Fig. 14c) for anchoring with a capacity up to 80% of the tensile strength of the pipe body. Since the connections used for this analysis are also proprietary and have 100% tensile efficiency, this allowed further PU loads of 50 klbf and 100 klbf to be applied to the upper MEP[1] and MEP[2], respectively. Ultimately, Fig. 14d shows the DLP for this cementless string, where the load cases due to AFE are not marginal in any loading region, benefiting from a 150 ft N_2 cap (34.6 bbl incremental AFE volume) in the pipe-in-pipe section and leak-off to formation fracture gradient in the pipe-in-hole section.

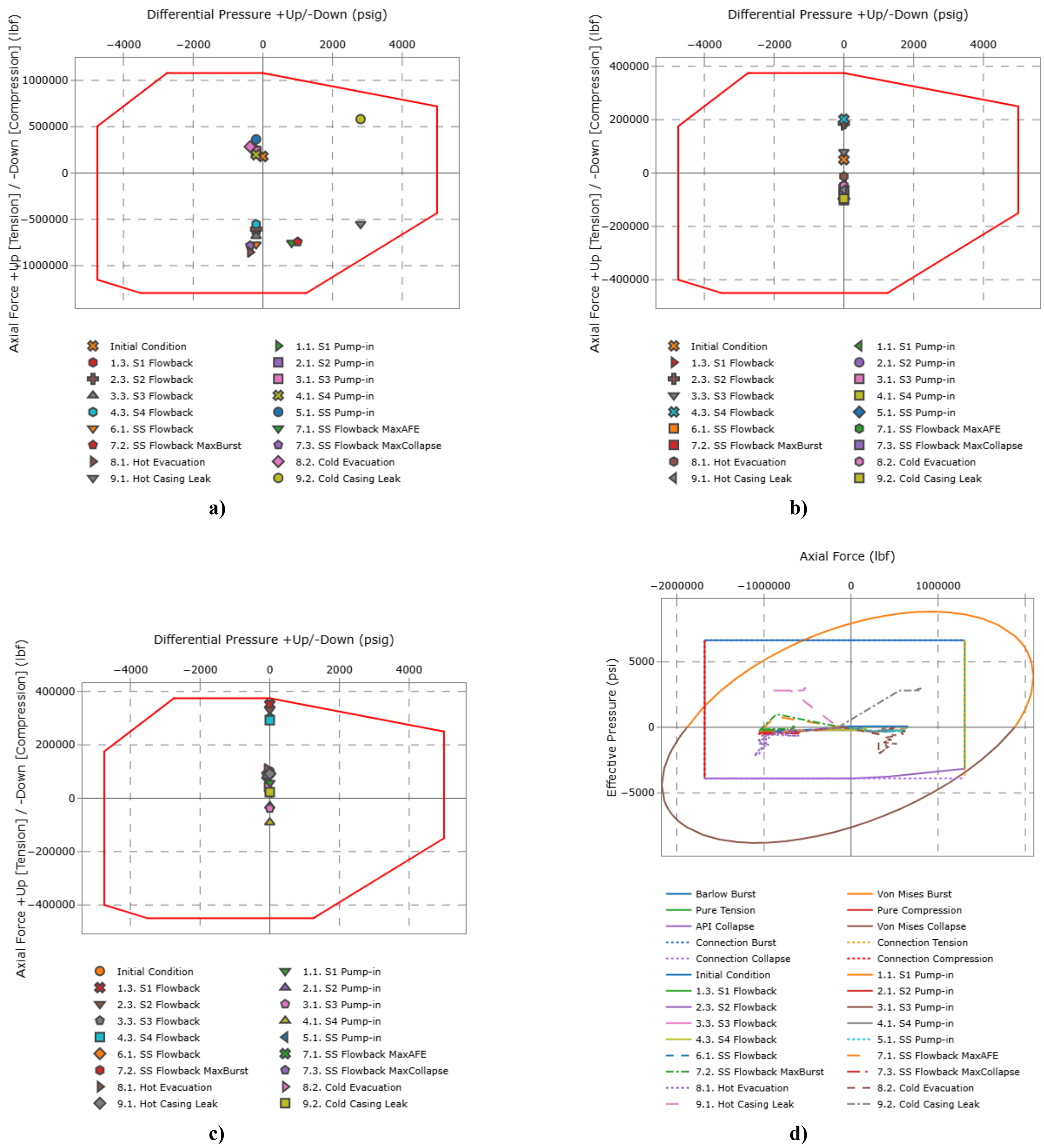

Figure 14: 11 ¾” cementless casing: a) WEA[1], b) 50 klbf PU on MEP[1], c) 100 klbf PU on MEP[2], d) DLP.

It is also interesting to evaluate the wellhead lift-off due to thermal expansion of the steel with and without cement. Thus, two scenarios are being compared in Fig. 15. The lift-off of the 11 ¾" casing head does not exceed an assumed default hanger lockdown rating of 500 klbf while a total of 150 klbf PU was locked between the packers (Fig. 15a). Although the 16" surface casing must be cemented as per the regulations, it may still be possible to apply a pre-tension up to 375 klbf to this string to reduce the wellhead growth and the lift-off force to below 500 klbf (Fig. 15b) when the 11 ¾" is cementless. However, if the 11 ¾" intermediate casing was cemented without any packers installed in the string, then the pre-tensioning must at least be 450 klbf to reduce the lift-off force below 500 klbf (Fig. 15c). Fig. 16 shows the resultant DLP of the 16" surface casing incorporating the maximum burst pressure build-up in the pipe-in-pipe section (11 ¾" x 16").

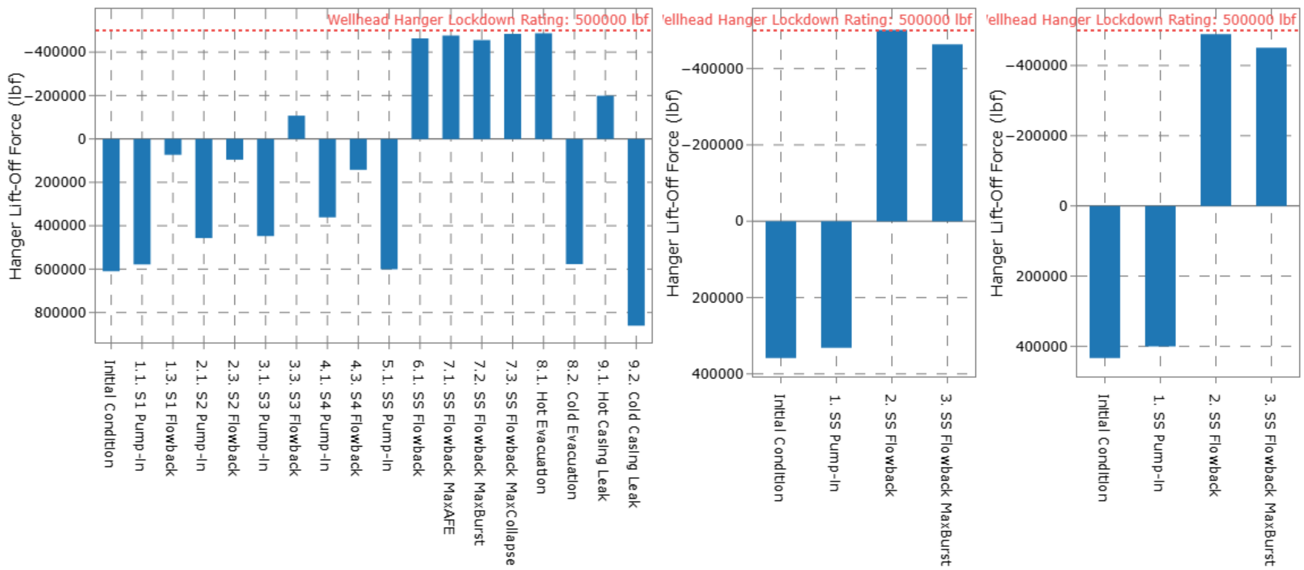

a) b) c)

Figure 15: Lift-off: a) 11 ¾" cementless intermediate casing with 50 klbf and 100 klbf PU on MEP[1] and MEP[2], respectively, b) 16" surface casing with 375 klbf PU on TOC (top of cement), while 11 ¾" is cementless, c) 16" surface casing with 450 klbf PU on TOC, while 11 ¾" is cemented.

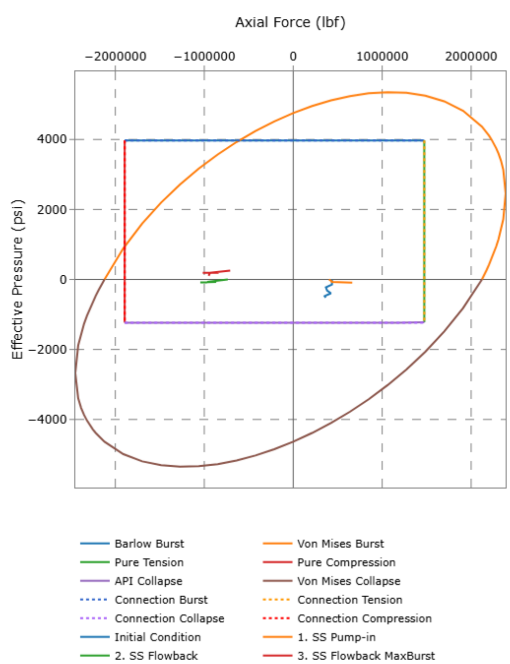

Figure 16: 16" cemented surface casing DLP.

4.2 Supercritical Hydrothermal Application

Since the compressive-tensile cycles are the main reasons why cement fails in geothermal wells, it is widely acknowledged that these wells must not be quenched abruptly. However, the main design philosophy behind an EGS application is to hydraulically fracture the subsurface formation that is suitable for enthalpy recovery. While it is hoped that pre-heated slickwater and/or polymer fluids are used for the stimulation of these wells, it is also acknowledged that the warm fracturing fluid may not serve the purpose of effectively creating a thermal shock to crack the tight rock. That was the main reason why a 90°F inlet temperature was used for the injection fluid in the evaluation of a cementless EGS application. As part of the study, it was also decided to evaluate the effectiveness of the cementless application in a supercritical hydrothermal application, which may not necessarily require a cold fracturing operation.

To begin with, the 7” production casing, which has the MEPs at the same depths as before, shows a safe working stress design in Fig. 17d. As before, the tubing-to-packer loads acting on the lowermost MEP[1] stay in the compressive region in the POE (Fig. 17a), as the quenching cool-down temperatures require more time to induce tensile loading on this packer. However, it can be seen from Fig. 17b that the cold shut-in and quenching load cases start to induce the tensile T_2P on MEP[2] with an applied 100 klbf PU load to reduce buckling, while this packer can still benefit from additional PU load if the POE and DLP allow.

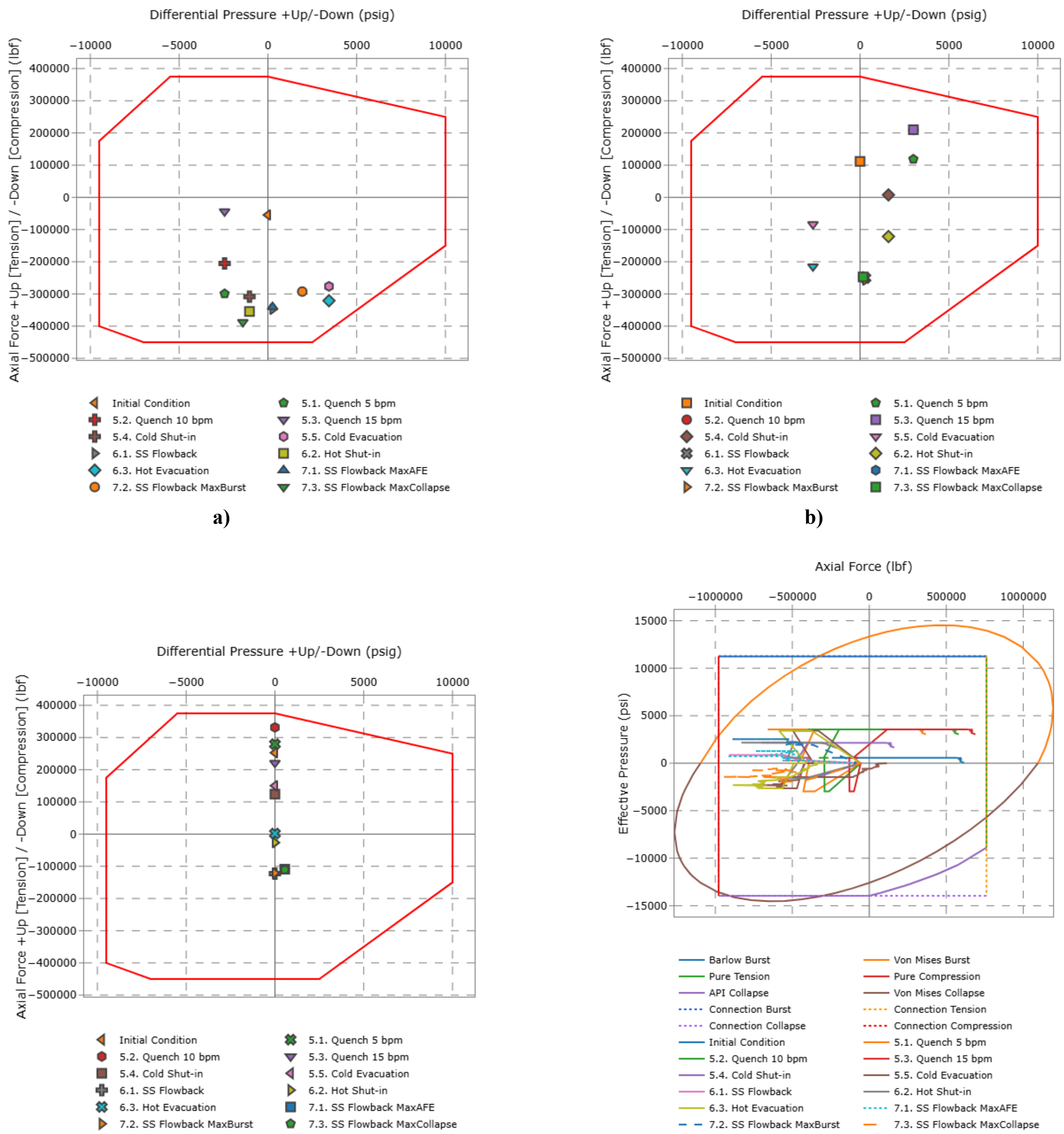

Figure 17: 7” cementless casing: a) MEP[1], b) 100 klbf PU on MEP[2], c) 100 klbf PU on MEP[3], d) DLP.

The uppermost packer, which is set inside the previous 11 ¾” casing near its shoe, undergoes a higher tensile T2P during the cold operations due to the applied PU load as well as the relatively quicker cold temperature evolution at shallower depths (Fig. 17c). It is also worth noting that a 1300 ft N_2 cap was simulated to reduce the amount of pressure build-up in the pipe-in-pipe (7” x 11 ¾”) section (i.e., incremental volume of 116.0 bbl), whereas the pressure build-up in the pipe-in-hole section was modeled to leak off into the formation fracture gradient, and the remaining pressure build-up was considered to act as a collapse load. This approach helped the AFE load cases stay inside the envelope (Fig. 17d). Although the producing temperatures are quite high, the lift-off analysis does not seem to be critical for the 7” casing string, also benefiting from a total applied PU load of 200 klbf (Fig. 18).

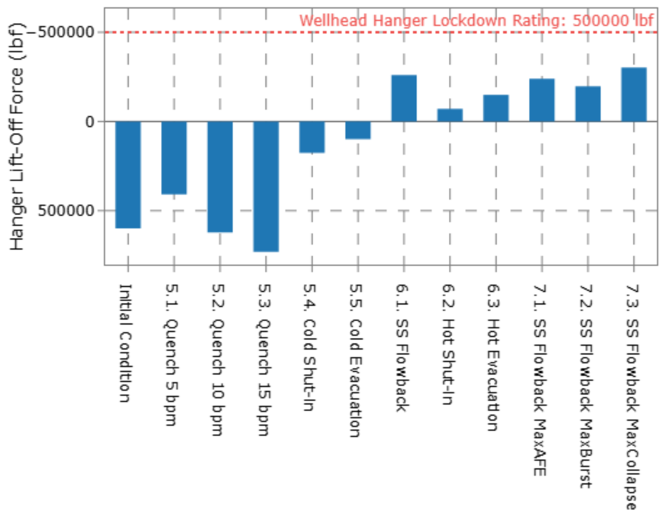

Figure 18: 7” cementless casing lift-off with 100 klbf PU on MEP[2] and 100 klbf PU on MEP[3].

Moving on to the previous 11 ¾” casing string and its packer components, it was decided to apply a PU load on the casing anchor to manage the compressive T_2P forces (Fig. 19a). As can be seen from Fig. 19a, the lowermost packer element has an applied and locked 300 klbf PU load, while an additional applied 200 klbf PU was decided to be applied on the uppermost MEP[2] (Fig. 19c), leaving MEP[1] neutral (Fig. 19b). However, it can be seen from Fig. 19d DLP that the load cases are marginal with the compression and burst ratings. Fig. 20, on the other hand, shows that the lift-off forces are higher than the assumed lockdown rating of 500 klbf. These results do not necessarily mean that the cementless design is not appropriate. Rather, it means that the study can benefit from a slightly modified approach while designing supercritical geothermal wells.

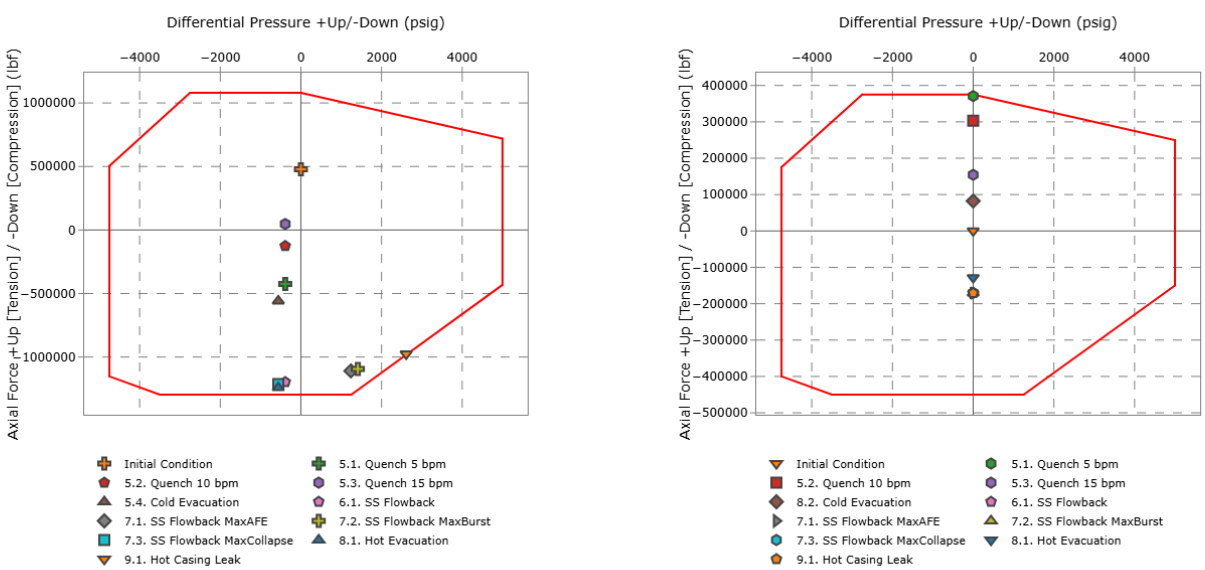

a)

b)

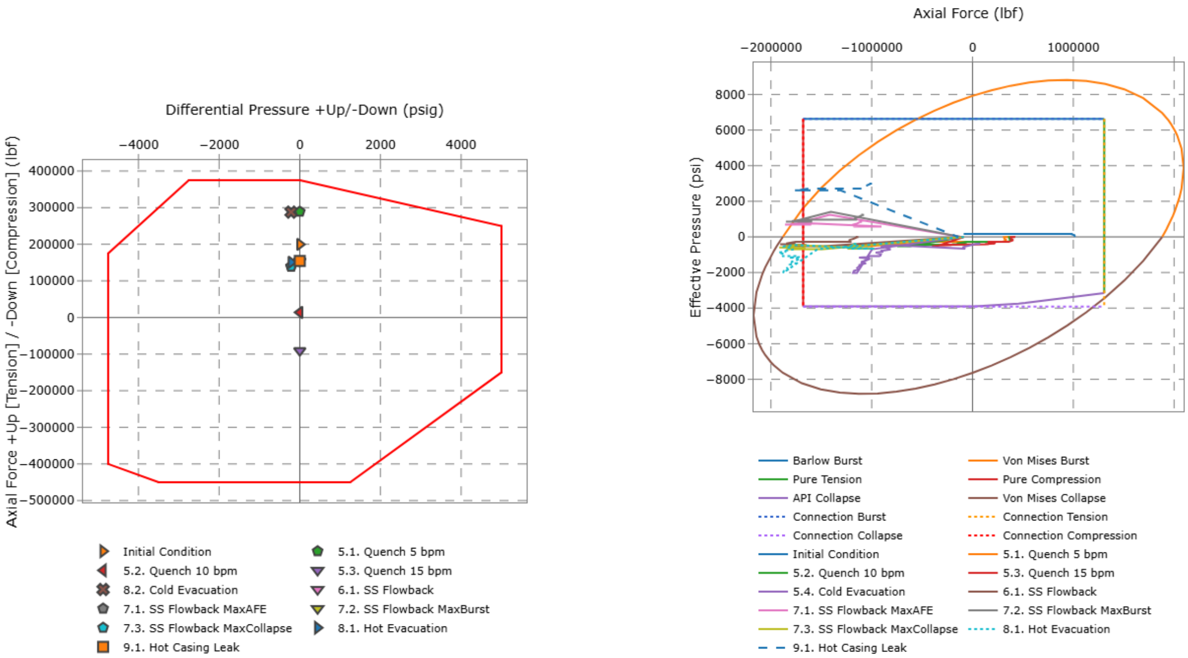

c) d)

Figure 19: 11 ¾" cementless casing: a) 300 klbf PU on WEA[1], b) MEP[1], c) 200 klbf PU on MEP[2], d) DLP.

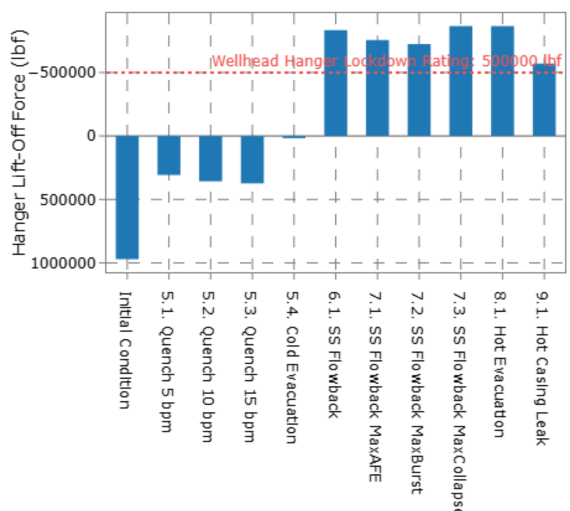

Figure 20: 11 ¾" cementless casing lift-off with 300 klbf PU on WEA[1] and 200 klbf PU on MEP[2].

As noted in the design philosophy section, the initial conditions for the cementless casing strings are assumed to be equivalent to casing running temperatures. While this is a reasonable assumption and a cementless design allows benefitting from additional circulation cool-down just before setting the packers, it does not necessarily mean that the initial conditions must be cold. The results of the evaluation study for the 11 ¾" just showed that the DLP has the load cases more dominant on the compression-burst quadrant. This can be mitigated by allowing the casing string to heat up just before setting the packers, which will lead to a lesser ΔT between the initial and the hot production conditions. This method of selecting the initial conditions should not be a universal practice; rather, it should be used to evaluate and fine-tune the operating conditions. Thus, it is understood that the 11 ¾" string can benefit from a heat-up before setting the packers, and in this case, it was assumed that the initial conditions' temperature profile is equivalent to UDT. This approach allowed a better-controlled PU load application and the loading conditions, as can be seen from Fig. 21d. It has been shown in Fig. 21a,b,c that the WEI[1], MEP[1], and MEP[2] all undergo a certain amount of PU load, which is managed and distributed better. Fig. 22 also shows that the lift-off forces are now minimized as much as possible (compared to the forces in Fig. 20). A 400 ft N_2 cap was simulated to reduce the amount of pressure build-up in the pipe-in-pipe (11 ¾" x 16") section (i.e., incremental volume of 33.2 bbl), whereas the pressure build-up in the pipe-in-hole section was modeled to leak off into the formation fracture gradient, and the remaining pressure build-up was considered to act as a collapse load. This approach helped the AFE load cases stay inside the envelope.

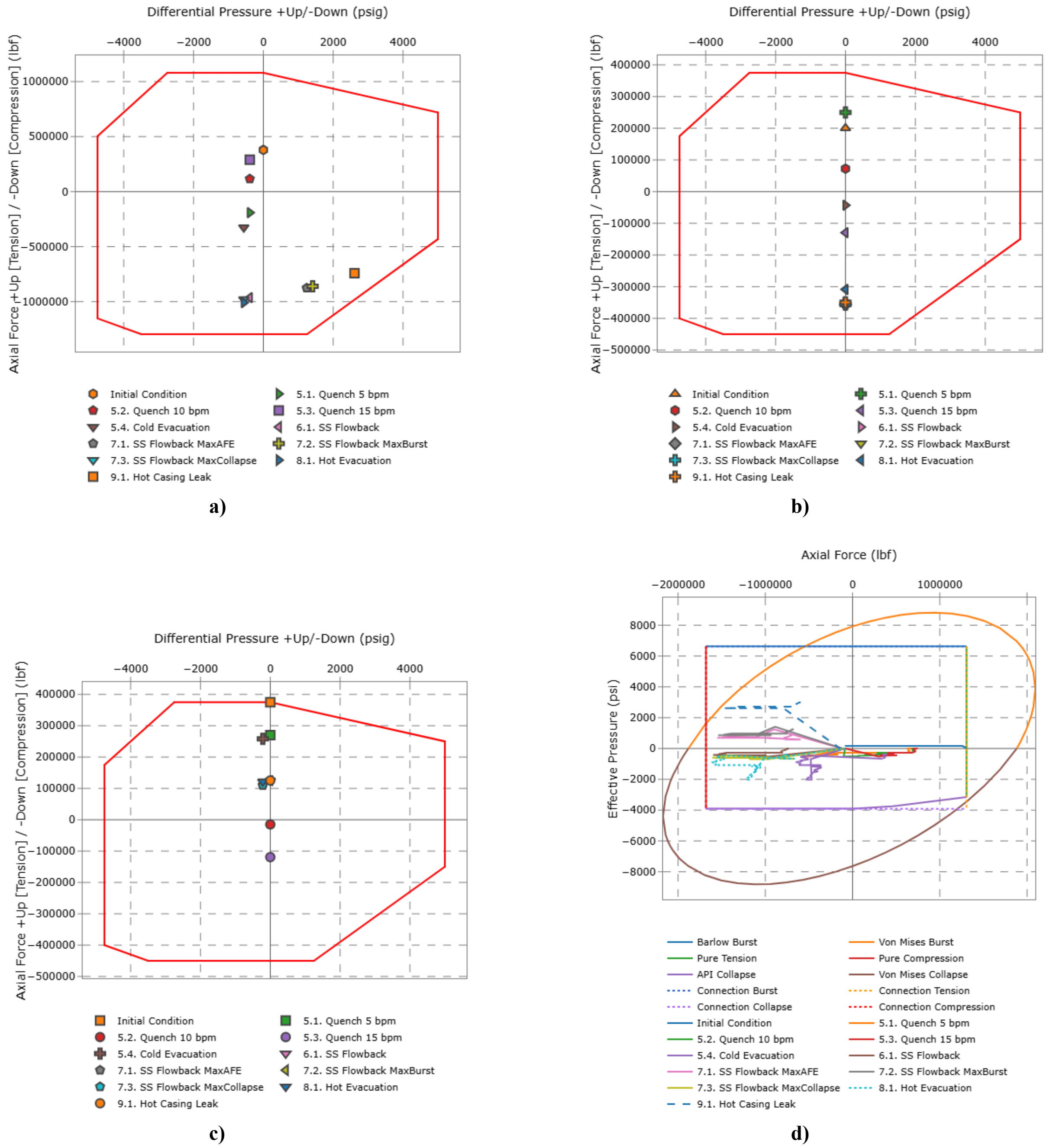

Figure 21: 11 ¾” cementless casing: a) 200 klbf PU on WEA[1], b) 200 klbf PU on MEP[1], c) 200 klbf PU on MEP[2], d) DLP.

However, it must be noted that the cemented 16” surface casing undergoes a substantial amount of compressive loads during hot production in this supercritical well. Even with a 500 klbf PU load on its TOC, the compressive lift-off forces reach as high as 1,500 klbf (Fig. 23b). It is acknowledged that the onshore wells’ surface casing must be cemented to the surface as per the regulations. An alternative option to reduce the lift-off forces acting on the wellhead would be to use thermal insulation between the 11 ¾” x 16” casing strings. Although the N_2 cap has been simulated as a mitigation solution for AFE and it has insulating properties, having a dedicated thermal insulation would be necessary for such high-temperature supercritical geothermal wells. It would also be beneficial to reduce the compressive loading on the 16” cemented surface casing (Fig. 23a).

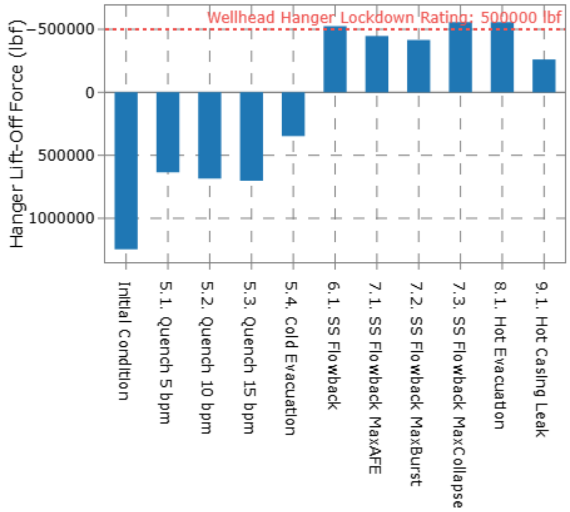

Figure 22: 11 ¾" cementless casing lift-off with 200 klbf PU on WEA[1], MEP[1], and MEP[2], respectively.

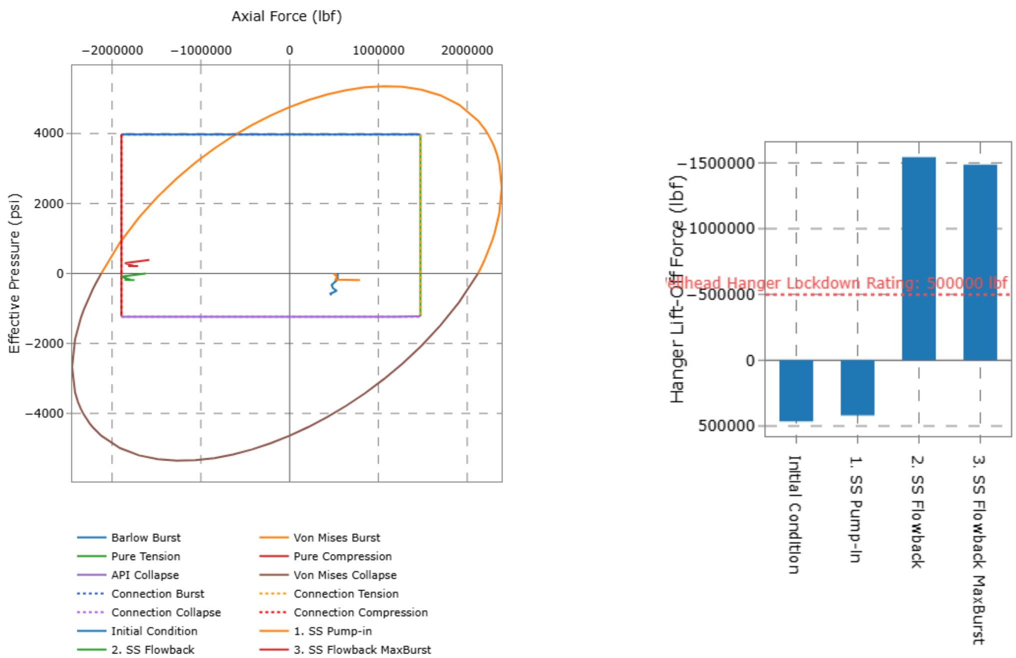

a) b)

Figure 23: 16" cemented casing with 500 klbf PU: a) DLP, b) lift-off.

5. DISCUSSIONS

The use of external casing packers has been suggested by Southon (2005), Shadravan et al. (2015) to provide a higher degree of certainty for the cement isolation quality, whereas these were inflatable or swell packers (Shadravan et al. 2015). Fast degradation of cement while in contact with the geothermal fluids, especially the CO_2 and H_2S, carbonation, micro-cracks, debonding, and deformation, and possibly arising interfacial damage during the high-pressure stimulation operations, and SCP issues necessitate a rethink of geothermal well construction and completion design philosophy. While the alternative cement formulations are significantly promising and their potential must not be underestimated, they are not without limitations of poor stability and weak performance in acidic and thermal cycling environments (Madirisha and Ikotun 2025), and there is a high chance that the deployment at the rig site may be hard to achieve in practice. Additionally, cemented casing strings do not enable SCP management, particularly in the pipe-in-pipe section, whereas the oil and gas industry already has experience managing pipe-in-pipe pressure buildup in HPHT wells. It is again worth noting that up to 70-80% of the high-temperature wells can suffer due to the SCP issues, a good portion of which might be due to cementing. Micro-annuli in a fully cemented geothermal well may be problematic because choke requirements to reduce production flow rate are often necessary, whereas high enthalpy recovery critically depends on flow rates. There may also be an onshore advantage of bleeding the annuli (or pressure relief valve), considering the pressure build-up in the pipe-in-pipe annuli. According to the design factor requirement for thermal expansion

(Union 2016) due to trapped fluid, the ratio of production casing collapse rating to surface casing burst rating should not be less than 1.2 (Marbun et al. 2020).

While a debonded casing-cement interface is a critical issue for inelastic buckling and cold collapse conditions, a cementless casing string may also buckle either sinusoidally or helically. No matter if the approach is cemented or cementless, the ideal practice would be implementing slow heat-up and cool-down in geothermal wells and potentially performing the fracturing with pre-heated fluid. However, further study needs to be done regarding the plastic buckling and deformation under the deployment with mini-packers and/or centralizers. It is worth noting that even if the ideal practices are implemented, a moderately small ΔT can induce tensile failures in cement, which lead to casing-cement interface debonding. This is backed by the fact that the cemented casings substantially reduce the number of cycles it takes for the interface debonding, whereas steel material can endure cycles ranging from 10 to 100s in terms of fatigue design in a range of less/more critical geothermal applications. An alternative would be allowing movement with the help of travel joints, which may need to be manufactured in a way that eliminates the concerns regarding the leak paths. Kaldal and Thorbjornsson (2022) explain the technology behind the flexible couplings (ISOR), which allow axial thermal expansion in high-temperature geothermal and thereby reduce the limitations concerning the plastic deformation of fully cemented casing strings (i.e., reducing the strain level to the elastic range). Additionally, wellhead movement (WHM) is more critical in cemented wells because of the widely used design assumption that the point-of-fixity (POF) is the top of the good cement. The problem gets more complicated if there is full cement to surface, but it has debonded, and there are frictional forces between the casing-cement interface, limiting the wellhead growth and lift-off. It needs to be noted that the WHM analysis is mostly ignored for the onshore wells, unless they are SAGD (steam-assisted gravity drainage) wells or there are offset well failures. However, a cementless approach can be more straightforward to apply a controlled PU load to the string and reduce the lift-off forces.

Hydrothermal high-temperature reservoirs can be more promising if the quenching is done in a controlled manner and can benefit from the expansion spool and growth allowance inside the wellhead; however, the EGS applications limit their usage due to stimulation operations, where the casing deformation failure frequency can range between 20-60% in hydraulically fractured fields, according to the statistics. Although most of these casing deformations are lateral and arise from geomechanical issues, plastic deformation in conjunction with thermal cycling is common in geothermal wells. It has been noted by Union (2016) that the geothermal wells are commonly completed in volcanic soils that present geomechanical instabilities as well. To be noted, the casing deformation failure frequency is 25-65% in the Sichuan and Qaidam basins of China, according to Lian et al. (2022), while in the Western Canada Sedimentary Basin and the USA, the amounts are 20-40% (Allen et al. 2019, McSpadden et al. 2025) and 20-30% (Jacobs 2020), respectively. According to Southon (2005), the casing failure rates for geothermal wells completed in Southeast Asia/Pacific in the 1990s were up to around 11% (McSpadden et al. 2025). Some deformation mechanisms of unconventional fractured wells have just started to attract proper attention, even though the industry has had more than a decade of hydraulic fracturing experience.

While the recent industry approach is to prefer the ductile strain-hardening grades instead of the high-strength steel, tensile fatigue cycles (up to 30-50 cycles depending on the material usage) must still be controlled carefully. To summarize, a broader question arises in relation to the functions of cement about what cement actually provides. It initially provides a certain protection against corrosion; however, since it degrades over time, and quite fast in high-temperature geothermal wells, a recommended further study would be to analyze the corrosion behavior in cemented and cementless casing strings. While it is straightforward to assume that the uniform corrosion would take place in a cementless string, it needs to be validated whether a damaged casing-cement interface undergoes higher localized corrosion than a cementless one. Unfortunately, this information was not readily available in the literature. It is worth noting that cementless can provide a benefit of controlling the corrosion in the external casing profile with the use of the feedthrough control lines. Another necessary further study would be the effectiveness of thermal insulation for the cementless, which can potentially reduce the compressive/tensile loading conditions for the outer strings, where N_2 is also beneficial for insulation. This study offered a reformist alternative to the industry practice of well cementing, acknowledging certain limitations and suggesting future studies.

6. CONCLUSIONS

This study aimed to demonstrate the suitability of a reformist well design philosophy for high-temperature EGS and supercritical hydrothermal geothermal wells, with inner strings deployed cementless (or cement-free). It has been shown that the approach offers a promising design methodology and outperforms cemented design in terms of wellhead movement and controlled SCP, enabled by controlled PU loads and N_2 in the pipe-in-pipe section. The pressure build-up in the pipe-in-hole section was modeled to leak off into the formation fracture gradient. Certain limitations related to buckling and corrosion have been discussed and suggested for further research, without advocating any single solution. However, it is still worth noting that the use/manufacture of proper centralizer tools and mini-packer/anchor systems can effectively reduce the buckling and help control it. Additionally, the external corrosion control can be achieved in a cementless design with the help of feedthrough control lines. As an integral part of the study, it has been shown how to effectively control the POEs by applying a specified amount of PU load, and comparisons were made with the cemented scenario where applicable.

ACKNOWLEDGEMENTS

The authors are deeply grateful to Altus Well Experts, Inc. for access to their PERIFOR™ software and permission to publish results. The successful completion of this study, particularly the detailed well design, was directly dependent on the software's advanced functionalities, which offered a robust and specialized alternative to other commercial finite element analysis (FEA) tools.

REFERENCES

Abid, Khizar, Baena, Felipe, Teodoriu, Catalin et al. 2025. Experimental Investigation of the Interfacial Debonding Strength of Class G Cement and the Implications to Well Integrity. International Journal of Greenhouse Gas Control 142: 104334. https://www.sciencedirect.com/science/article/pii/S1750583625000325.

Abdullah, Muhammad and Sajjadi, Baharak. 2024. Sustainable Conversion of Natural Gas to Hydrogen Using Transition Metal Carbides. International Journal of Hydrogen Energy 90: 61-103. https://www.sciencedirect.com/science/article/pii/S0360319924040795.

Ahmed, Ramadan, Salehi, Saeed, and Srivastava, Aman. 2022. Evaluation of Hydroxyapatite-Based Cement for Geothermal Well Applications. Geothermics 104: 102462. https://www.sciencedirect.com/science/article/pii/S0375650522001122.

Allahverdiyev, Elvin, Abid, Khizar, and Teodoriu, Catalin. 2025. Post-Well Construction Service-Life Model Design of Utah FORGE Enhanced Geothermal Systems. GRC Transactions 49. https://publications.mygeoenergynow.org/grc/TV49.pdf.

Allahvirdizadeh, Payam. 2020. A Review on Geothermal Wells: Well Integrity Issues. Journal of Cleaner Production 275: 124009. https://www.sciencedirect.com/science/article/pii/S0959652620340543.

Allen, D, Eberhardt, E, and Bustin, A. 2019. Scientific Review of Hydraulic Fracturing in British Columbia. Report of the Scientific Hydraulic Fracturing Review Panel (Reprint).

Arbad, Nachiket, Emadi, Hossein, and Watson, Marshall. 2022. A Comprehensive Review of Geothermal Cementing from Well Integrity Perspective. Journal of Petroleum Science and Engineering 217: 110869. https://www.sciencedirect.com/science/article/pii/S0920410522007252.

Baig, Abdul Rehman, Fentaw, Jemal, Hajiyev, Elvin et al. 2025. Comprehensive Insights into Carbon Capture and Storage: Geomechanical and Geochemical Aspects, Modeling, Risk Assessment, Monitoring, and Cost Analysis in Geological Storage. Sustainability 17 (19): 8619. https://www.mdpi.com/2071-1050/17/19/8619.

Berndt, Marita L and Philippacopoulos, Aristodimos J. 2002. Incorporation of Fibres in Geothermal Well Cements. Geothermics 31 (6): 643-656.

Bett, Evans. 2017. Geothermal Well Cementing, Materials and Placement Techniques: LAP Lambert Academic Publishing.

Carter, Greg and Smith, Dwight K. 1958. Properties of Cementing Compositions at Elevated Temperatures and Pressure. Transactions of the AIME 213 (01): 20-27.

Code of Practice for Deep Geothermal Wells (NZS 2403: 2015), 2015.

England, Kevin. 2024. Utah FORGE: Wells 16A(78)-32 and 16B(78)-32 Stimulation Pressure and Circulation Data April, 2024, Energy and Geoscience Institute at the University of Utah (Reprint). https://doi.org/10.15121/2371032.

Fentaw, Jemal Worku, Hajiyev, Elvin, Baig, Abdul Rehman et al. 2026. Coupling Geothermal Energy with Geological Carbon Storage: A Holistic Review of Enhanced Geothermal Systems Using CO_2 as a Working Fluid. Next Energy 10: 100486. https://www.sciencedirect.com/science/article/pii/S2949821X25002492.

Ford, Eric P, Majoumerd, Mohammad Mansouri, Randeberg, Erlend et al. 2017. Barrier Definitions and Risk Assessment Tools for Geothermal Wells. H2020-GeoWell report.

Garnier, A., Saint-Marc, J., Bois, A. -P. et al. 2008. A Singular Methodology to Design Cement Sheath Integrity Exposed to Steam Stimulation. Proc., International Thermal Operations and Heavy Oil Symposium. https://doi.org/10.2118/117709-MS.

GHG, IEA. 2006. 2nd Well Bore Integrity Workshop.

Gu, Chenwang, Feng, Yongcun, Mosleh, Mojgan Hadi et al. 2024. Fluid-Driven Debonding of Cement Interfaces of an Injector Well: A Coupled Thermo–Hydro–Mechanical Approach. Rock Mechanics and Rock Engineering 57 (7): 4513-4531.

Gu, Chenwang, Li, Xiaorong, Feng, Yongcun et al. 2022. Numerical Investigation of Cement Interface Debonding in Deviated Shale Gas Wells Considering Casing Eccentricity and Residual Drilling Fluid. International Journal of Rock Mechanics and Mining Sciences 158: 105197.

Hajiyev, Elvin, Watson, Marshall, Emadi, Hossein et al. 2025. A Comparative Study of Major Risk Assessment (RA) Frameworks in Geologic Carbon Storage (GCS). Fuels 6 (2): 42.

Hole, Hagen. 2008a. Geothermal Well Cementing. Petroleum Engineering Summer School, Dubrovnik, Croatia: Petroleum Engineering Summer School.

Hole, Hagen. 2008b. Geothermal Well Design - Casing and Wellhead. Proc., Petroleum Engineering Summer School Workshop9-13.

Jacobs, Trent. 2020. An Unconventional Challenge Can Casing Failures During Hydraulic Fracturing Be Stopped? Journal of Petroleum Technology 72 (01): 26-32.

Jiang, Jiwei, Li, Jun, Liu, Gonghui et al. 2020. Numerical Simulation Investigation on Fracture Debonding Failure of Cement Plug/Casing Interface in Abandoned Wells. Journal of Petroleum Science and Engineering 192: 107226.

Johri, Ambuj, Johnson, Carl R., Rasheed, Hassaan et al. 2025. Cementing in Thermal Wells: A Three-Pronged Approach to Well Integrity. Proc., SPE Thermal Well Integrity and Production Symposium. https://doi.org/10.2118/230275-MS.

Kaldal, Gunnar Skúlason and Thorbjornsson, IO. 2022. Improved Integrity of the Production Casing in Moderate-to Ultra-High-Temperature Geothermal Wells using Flexible Couplings. Geothermal Resources Council Transactions 46: 256-270.

Lambrescu, Ionut, Abid, Khizar, and Teodoriu, Catalin. 2024. Cement-Formation Debonding Due to Temperature Variation in Geothermal Wells: An Intensive Numerical Simulation Assessment. Energies 17 (19): 4953.

Lambrescu, Ionut, Allahverdiyev, Elvin, Abid, Khizar et al. 2025. Numerical Modeling of Casing-Cement Failure in Geothermal Wells Using Modified CZM Bonding Conditions.

Lambrescu, Ionut and Teodoriu, Catalin. 2022. Experimental and Numerical Investigations of Cement Bonding Properties at Elevated Temperatures—The Effect of Sample Cooling. Materials 15 (14): 4955. https://www.mdpi.com/1996-1944/15/14/4955.

Lambrescu, Ionut, Teodoriu, Catalin, and Amani, Mahmood. 2021. Experimental and Numerical Investigations of Cement Bonding Properties. Materials 14.

Lentsch, David, Dorsch, Klaus, Sonnleitner, Natascha et al. 2015. Prevention of Casing Failures in Ultra-Deep Geothermal Wells (Germany). Prevention 19: 25.

Lian, Wei, Li, Jun, Tao, Qian et al. 2020. Formation Mechanism of Continuous Gas Leakage Paths in Cement Sheath During Hydraulic Fracturing. Energy Science & Engineering 8 (7): 2527-2547.

Lian, Wei, Liu, Jiayi, He, Yu et al. 2022. Distribution Characteristics and Cause Analysis of Casing Deformation during Hydraulic Fracturing of Shale Gas Wells. Processes 10 (11): 2421.

Liu, Kui, Gao, Deli, and Taleghani, Arash Dahi. 2018. Analysis on Integrity of Cement Sheath in the Vertical Section of Wells During Hydraulic Fracturing. Journal of Petroleum Science and Engineering 168: 370-379. https://www.sciencedirect.com/science/article/pii/S092041051830408X.

Liu, Shuai, Zhang, Chunmei, Hu, Chen et al. 2025. Study on Low Thermal Conductivity Cement Reinforced by Sepiolite Fiber for Deep Geothermal Well. Geothermics 129: 103290. https://www.sciencedirect.com/science/article/pii/S0375650525000422.

Madirisha, Makungu M and Ikotun, Bolanle D. 2025. The Future of Geothermal Wellbore Integrity: Geopolymer Cements for Enhanced Stability and Hydrogen Coproduction. International Journal of Energy Research 2025 (1): 6641119.

Maharaj, G. 1996. Thermal Well Casing Failure Analysis. Proc., SPE Latin America/Caribbean Petroleum Engineering Conference. https://doi.org/10.2118/36143-MS.

Marbun, B. T. H., Ridwan, R. H., Nugraha, H. S. et al. 2020. Casing Setting Depth and Design of Production Well in Water-Dominated Geothermal System with 330 °C Reservoir Temperature. Energy Reports 6: 582-593. https://www.sciencedirect.com/science/article/pii/S235248471930352X.

McLennan, John, Mock, Blake, Swearingen, Leroy et al. 2023. Utah FORGE: Well 16B(78)-32 Drilling Data, Energy and Geoscience Institute at the University of Utah (Reprint). https://doi.org/10.15121/1998591.

McSpadden, Albert R, Coker, Oliver D, and Bohlander, Spencer. 2025. Closed-Loop Geothermal Well Design: Simulation Study of Intermittent Circulation and Thermal Soak Times. SPE Journal: 1-21.

Muehlenbachs, Karlis. 2011. Identifying the Sources of Fugitive Methane Associated with Shale Gas Development. Resources For the Future, Washington, DC 14.

Patel, Zishan Mubarak, Mahmoud, Ahmed Abdulhamid, and Wang, Yuzhu. 2025. Improvement in Geothermal Well Integrity: A Review of New Advanced Cementing Technologies. Proc., Middle East Oil, Gas and Geosciences Show (MEOS GEO). https://doi.org/10.2118/227610-MS.

Petty, Susan, Gastineau, John, Bour, Daniel L et al. 2003. Life Cycle Modeling of Wellbore Cement Systems Used for Enhanced Geothermal System Development. Proc., 28th Workshop on Geothermal Reservoir Engineering, Stanford U.(27–29 January 2003).

Phi, Thai, Elgaddafi, Rida, Al Ramadan, Mustafa et al. 2019. Well Integrity Issues: Extreme High-Pressure High-Temperature Wells and Geothermal Wells A Review. Proc., SPE Thermal Well Integrity and Design Symposium. https://doi.org/10.2118/198687-MS.

Pyatina, Tatiana and Sugama, Toshifumi. 2020. Cements with Supplementary Cementitious Materials for High-Temperature Geothermal Wells. Geothermics 86: 101840.

Pyatina, Tatiana and Sugama, Toshifumi. 2022. Self-Healing and Crack-Sealing Ability of 30-Day-Long 300°C Cured Thermal Shock Resistant Cement Composites. Geothermal Resource Council 43: 1125-1149.

Pyatina, Tatiana, Sugama, Toshifumi, and Ronne, A. 2016. Self-Repairing Geothermal Well Cement Composites. GRC Transactions 40: 235-244.

Radonjic, Mileva and Bello, Kolawole S. 2015. Experimental Assessment of Cement Integrity under Geopressured Geothermal Reservoir Conditions. Proc., World Geothermal Congress.

Ravi, K., Fukuzawa, M., Hunter, W. J. et al. 2008. Advanced Cement Systems Used to Improve Geothermal Well Reliability in Java. Proc., SPE Annual Technical Conference and Exhibition. https://doi.org/10.2118/115638-MS.

Saito, Seiji. 1994. A New Advanced Method for Top-Job Casing Cementing. Transactions-Geothermal Resources Council: 99-99.

Salim, Prisca and Amani, Mahmood. 2013. Principal Points in Cementing Geothermal Wells. Advances in Petroleum Exploration and Development 5 (1): 77-91.

Santos, Livio and Dahi Taleghani, Arash. 2022. On Quantitative Assessment of Effective Cement Bonding to Guarantee Wellbore Integrity. Journal of Energy Resources Technology 144 (1): 013001.

Saunders, Calvin D and Walker, Wayne A. 1954. Strength of Oil Well Cements and Additives under High Temperature Well Conditions. Proc., SPE Annual Technical Conference and Exhibition? SPE-390-G.

Shadravan, Arash, Ghasemi, Mohammadreza, and Alfi, Mehrdad. 2015. Zonal Isolation in Geothermal Wells. Proc., Fortieth Workshop on Geothermal Reservoir Engineering26-28.

Southon, James NA. 2005. Geothermal Well Design, Construction and Failures. *Proc.,* Proceedings World Geothermal Congress, April, 24-29.

Subsurface Data, https://utahforge.com/data/ (accessed October 2, 2025).

Sugama, Toshifumi and Pyatina, Tatiana. 2019. Self-Healing, Re-adhering, and Corrosion-Mitigating Inorganic Cement Composites for Geothermal Wells at 270°-300°C: Final Report, BNL--211405-2019-INRE, Brookhaven National Laboratory (BNL), Upton, NY (United States), United States.

Swearingen, Leroy. 2024a. Utah FORGE: Daily Reports for the 2024 Stimulation of Wells 16A/16B(78)-32, Energy and Geoscience Institute at the University of Utah (Reprint). https://doi.org/10.15121/2440866.

Swearingen, Leroy. 2024b. Utah FORGE: Wells 16A(78)-32 and 16B(78)-32 Circulation Test Daily Reports from August 2024, Energy and Geoscience Institute at the University of Utah (Reprint). https://doi.org/10.15121/2455019.

Teodoriu, Catalin. 2021. A Discussion on Geothermal Well Integrity using Long Term Experimental Bonding and Re-Bonding Data. Proc., Proceedings, 46th Workshop on Geothermal Reservoir Engineering, Stanford University, Stanford, California.

Teodoriu, Catalin, Bello, Opeyemi, Vasquez, R. R. et al. 2021. Cementless Well Construction Opens the Full Control on Well Integrity for the Life of the Well. Proc., SPE Annual Technical Conference and Exhibition. https://doi.org/10.2118/206052-MS.

Teodoriu, Catalin, Esquitin, Yosafat, and Vasques, Ricardo. 2022. Can Geothermal Wells Go Cementless. Proc., 47th Workshop on Geothermal Reservoir Engineering; Stanford University: Stanford, CA, USA.

Teodoriu, Catalin and Lambrescu, Ionut. 2023. Numerical Investigations of Tensile Induced Debonding Due To Temperature Variation in Geothermal Wells. Proc., 48th Workshop on Geothermal Reservoir Engineering. Stanford University: Stanford University.

Tomilina, Elena M., Chougnet-Sirapian, Alice, and Aboutourkia, Wesam. 2012. New Thermally Responsive Cement for Heavy Oil Wells. Proc., SPE Heavy Oil Conference Canada. https://doi.org/10.2118/157892-MS.

The African Union Code of Practice for Geothermal Drilling, 2016.

Ugwu, Ignatius Obinna. 2009. Cement Fatigue and HPHT Well Integrity with Application to Life of Well Prediction.

Vengosh, Avner, Jackson, Robert B, Warner, Nathaniel et al. 2014. A Critical Review of the Risks to Water Resources from Unconventional Shale Gas Development and Hydraulic Fracturing in the United States. Environmental Science & Technology 48 (15): 8334-8348.

Vu, Manh-Huyen, Bois, Axel-Pierre, and Badalamenti, Anthony M. 2020. Cement Mechanical Integrity for Geothermal Wells. Transactions-Geothermal Resources Council 44: 129-142.

Williams, H, Khatri, D, Keese, R et al. 2011. Flexible, Expanding Cement System (FECS) Successfully Provides Zonal Isolation across Marcellus Shale Gas Trends. Proc., SPE Canada Unconventional Resources Conference SPE-149440-MS.

Wu, Yuxing, Patel, H, and Salehi, Saeed. 2020. Thermal Considerations of Cement Integrity in Geothermal Wells. Proc., The 45th Workshop on Geothermal Reservoir Engineering. Stanford, California, USA.

Wu, Yuxing, Patel, Harshkumar, and Salehi, Saeed. 2021. Parametric Study of Mechanical Stresses within Cement Sheath in Geothermal Wells. Geothermics 90: 102000. https://www.sciencedirect.com/science/article/pii/S0375650520302923.

Xi, Yan, Jin, Jianzhou, Fan, Lifeng et al. 2022. Research on the Establishment of Gas Channeling Barrier for Preventing SCP Caused by Cyclic Loading-Unloading in Shale Gas Horizontal Wells. Journal of Petroleum Science and Engineering 208: 109640.

Xu, Honglin, Peng, Nian, Ma, Tianshou et al. 2018. Investigation of Thermal Stress of Cement Sheath for Geothermal Wells during Fracturing. Energies.

Yao, Theodore and Wojtanowicz, Andrew. 2017. Criteria and Risk of Integrity Loss for Wells with Sustained Casing Pressure. AGH Drilling, Oil, Gas 34 (2): 639-654.

Yin, Yue, Zhang, Li-Wei, Mei, Kai-Yuan et al. 2025. CT Investigation on Oilwell Cement Deterioration Caused by H2S along a Leaking Channel under High Temperature: Insights for Geothermal Applications. Petroleum Science. https://www.sciencedirect.com/science/article/pii/S1995822625004819.

Yin, Yue, Zhang, Liwei, Mei, Kaiyuan et al. 2024. Experimental Investigation on H2S-Induced Oilwell Cement Degradation Under High-Temperature Conditions for Geothermal Applications. Geothermics 121: 103023. https://www.sciencedirect.com/science/article/pii/S0375650524001123.

Zhang, Zhi, Xiang, Shilin, Yang, Huabo et al. 2024. Study on the Integrity Assessment of Geothermal Wellbore under Thermal and Non-Uniform In-Situ Stresses Coupling Effects. Applied Thermal Engineering 255: 123744. https://www.sciencedirect.com/science/article/pii/S1359431124014121.

APPENDIX

Table 2: Post-installation stimulation and life-of-well operational loads, modified after Swearingen (2024b), England (2024), Swearingen (2024a).

Stage	Operations	WHP (psi)	7" WHT (°F)	11 ¾" WHT (°F)	Average Flow Rate (bpm)	Duration
1	Pump-in	7,460	90*	75	53.2	71 min.
	Shut-in	4,340	88	-	-	15 min.
	Flowback	1,730	282	147	2.0	1,410 min.
2	Pump-in	7,500	90*	131	55.7	88 min.
	Shut-in	4,660	96	-	-	15 min.
	Flowback	2,680	266	152	1.7	1,410 min.
3	Pump-in	7,880	90*	136	50.7	88 min.
	Shut-in	3,740	97	-	-	15 min.
	Flowback	1,710	338	194	4.5	945 min.
4	Pump-in	5,350	90*	171	56.1	70 min.
	Shut-in	3,340	104	-	-	15 min.
	Flowback	1,610	238	154	1.1	1,875 min.
1-4**	Steady-State (SS) Pump-in	3,000	90*	83	10.0	20 years**
	Cold Shut-in	1,600	82	-	-	1 day**
	Cold Evacuation	0	82	83	-	-
	Cold Casing Leak***	3,000	-	83	10	-
1-4**	Steady-State (SS) Flowback	300	387	309	8.95	20 years**
	Hot Shut-in	1,600	246	-	-	1 day**
	Hot Evacuation	0	246	309	-	-
	Hot Casing Leak***	3,000	-	309	-	-
*Increased the max. monthly average inlet temperature to reduce the damage from cold tensile loads						
**Assumed life-of-well loads and completion interval						
***Leak into the previous casing						

Table 3: Post-installation stimulation and life-of-well operational loads, modified after Swearingen (2024b), England (2024), Swearingen (2024a).

Stage	Operations	WHP (psi)	7” WHT (°F)	11 ¾” WHT (°F)	Average Flow Rate (bpm)	Duration
N/A	Quench	3,000	90	236	5	1 hour
	Quench	3,000	90	236	10	1 hour
	Quench	3,000	90	236	15	1 hour
	Cold Shut-in	1,600	199	-	-	1 day
	Cold Evacuation	0	199	189	-	-
	SS Flowback	300	586	507	8.95	20 years
	Hot Shut-in	1,600	338	-	-	1 day
	Hot Evacuation	0	338	507	-	-
	Hot Casing Leak*	3,000	-	507	10	-
*Leak into the previous casing						